NAVAL POSTGRADUATE SCHOOL

Monterey, California

THESIS

PROPAGATION OF SOUND
IN
A LAYERED LABORATORY MODEL

by

Mohammad Tariq
and
Suttichai Rungsirotekomol

December 1984

Thesis Advisor: James V. Sanders

SECURITY CLASSIFICATION OF THIS PAGE (When Data Entered)

REPORT DOCUMENTATION PAGE

READ INSTRUCTIONS BEFORE COMPLETING FORM

1. REPORT NUMBER

2. GOVT ACCESSION NO.

3. RECIPIENT'S CATALOG NUMBER

4. TITLE (and Subtitle)
Propagation of Sound
in
a Layered Laboratory Model

5. TYPE OF REPORT & PERIOD COVERED
Master's Thesis;
December 1984

6. PERFORMING ORG. REPORT NUMBER

7. AUTHOR(s)
Mohammad Tariq
and
Suttichai Rungsirotekomol

8. CONTRACT OR GRANT NUMBER(s)

9. PERFORMING ORGANIZATION NAME AND ADDRESS
Naval Postgraduate School
Monterey, California 93943

10. PROGRAM ELEMENT, PROJECT, TASK AREA & WORK UNIT NUMBERS

11. CONTROLLING OFFICE NAME AND ADDRESS
Naval Postgraduate School
Monterey, California 93943

12. REPORT DATE
December 1984

13. NUMBER OF PAGES
75

14. MONITORING AGENCY NAME & ADDRESS(if different from Controlling Office)

15. SECURITY CLASS. (of this report)
UNCLASSIFIED

15a. DECLASSIFICATION/ DOWNGRADING SCHEDULE

16. DISTRIBUTION STATEMENT (of this Report)
Approved for public release; distribution unlimited

17. DISTRIBUTION STATEMENT (of the abstract entered in Block 20, if different from Report)

18. SUPPLEMENTARY NOTES

19. KEY WORDS (Continue on reverse side if necessary and identify by block number)
Sound Propagation
Shallow Water
Normal Modes
Shallow Water Facility

20. ABSTRACT (Continue on reverse side if necessary and identify by block number)

The propagation of sound in a laboratory model consisting of a surface layer of water overlying a thick bottom layer of sand was experimentally investigated. The variations of pressure amplitude as a function of receiver depth, range, and transverse location were measured for the source at constant depth in the surface layer of water. Three frequencies for which only the lowest mode propagates were

DD FORM 1 JAN 73 1473 EDITION OF 1 NOV 65 IS OBSOLETE
S N 0102-LF-014-6601

SECURITY CLASSIFICATION OF THIS PAGE (When Data Entered)

used in this investigation. The measurements of pressure amplitude as a function of depth and range were found in good agreement with normal mode theory, when absorption in the bottom was taken into consideration.

Approved for public release; distribution is unlimited.

Propagation of Sound in a Layered Laboratory Model

by

Mohammad Tariq
Lieutenant Commander, Pakistan Navy
M.Sc(Physics) University of Punjab Lahore(Pakistan), 1972

and

Suttichai Rungsirotekomol
Ensign, Royal Thai Navy
B.S., Royal Thai Naval Academy, 1980

Submitted in partial fulfillment of the
requirements for the degree of

MASTER OF SCIENCE IN ENGINEERING ACOUSTICS

from the

NAVAL POSTGRADUATE SCHOOL
December 1984

ABSTRACT

The propagation of sound in a laboratory model consisting of a surface layer of water overlying a thick bottom layer of sand was experimentally investigated. The variations of pressure amplitude as a function of receiver depth, range, and transverse location were measured for the source at constant depth in the surface layer of water. Three frequencies for which only the lowest mode propagates were used in this investigation. The measurements of pressure amplitude as a function of depth and range were found in good agreement with normal mode theory, when absorption in the bottom was taken into consideration.

TABLE OF CONTENTS

LIST OF TABLES

LIST OF FIGURES

ACKNOWLEDGEMENT

We are deeply indebted to Professor James V. Sanders and Professor Allan B. Coppens of the Department of Physics, U.S. Naval Postgraduate School for their invaluable guidance and immense help in our theoretical and experimental work as well as in editing of this thesis. We would also like to express our profound gratitudes to Dr. F. H. Fisher for providing Postgraduate School an opportunity to use the tank, without which we would not have been able to conduct our experiments. We will be failing in our duty if we do not acknowledge the support and assistance rendered by Kerry Yarber, Steve Philip, Lyn May, Bob Moller, and Gene Wall of the Department of Physics for facilitating the orderly arrangements for our experiments. Finally we would like to thank Mrs. Chanida Rungsirotekomol for the tremendous effort she put in, in typing the manuscript of this thesis.

I. PROPAGATION OF SOUND IN THE HOMOGENOUS LAYERED MODEL

The transmission of sound in the ocean is dependent on several environmental factors. The most important of these include the depth, the nature of the bottom, sound velocity structure within the ocean, and the shape of ocean bottom and surface. The purpose of this experiment was to investigate the propagation of sound in a two layered laboratory model, composed of sand and water. In this study the bottom and surface of the model were made flat and experimental results were compared with a simple theoretical model.

II. PROPAGATION OF SOUND IN SHALLOW WATER

A. INTRODUCTION

The propagation of sound in shallow water is a complicated problem, involving multiple reflections of the sound between the surface and the bottom, so that there is considerable phase interference among the various multipaths. At relatively long ranges, the sound field is mainly due to the multiple reflections. The transmission of sound in the shallow water also depends on several environmental factors: nature and slope of the bottom, depth of water relative to wave length, roughness of surface and bottom and temperature gradient. As a consequence of the multiplicity of reflections from the surface and the bottom and the environmental factors, the predictions of sound transmission in shallow water can be much more complicated than for deep water. Ray theory can be used for the sound field at short range when the depth of the water is relatively large. But, ray theory has limited applications. It is inapplicable in a shadow zone. Ray theory also cannot be used for low frequencies when the wavelength of sound becomes comparable with the vertical scale of sound velocity variation. Therefore, in practice one ultimately has to resort to a wave solution of the problem.

B. NORMAL MODES IN TWO HOMOGENOUS LAYERS

Normal mode theory provides an exact solution to the wave equation and is also useful for dealing with depth dependent sound profile particularly those leading to the trapping of sound. There are various approaches to the normal mode theory but we will use the

eigenfunction-expansion technique, which is relatively simple. In this presentation we will follow mainly [Ref. 1] and [Ref. 2].

Consider the case of two homogeneous layers with a pressure release surface above as shown in Figure 2.1 .

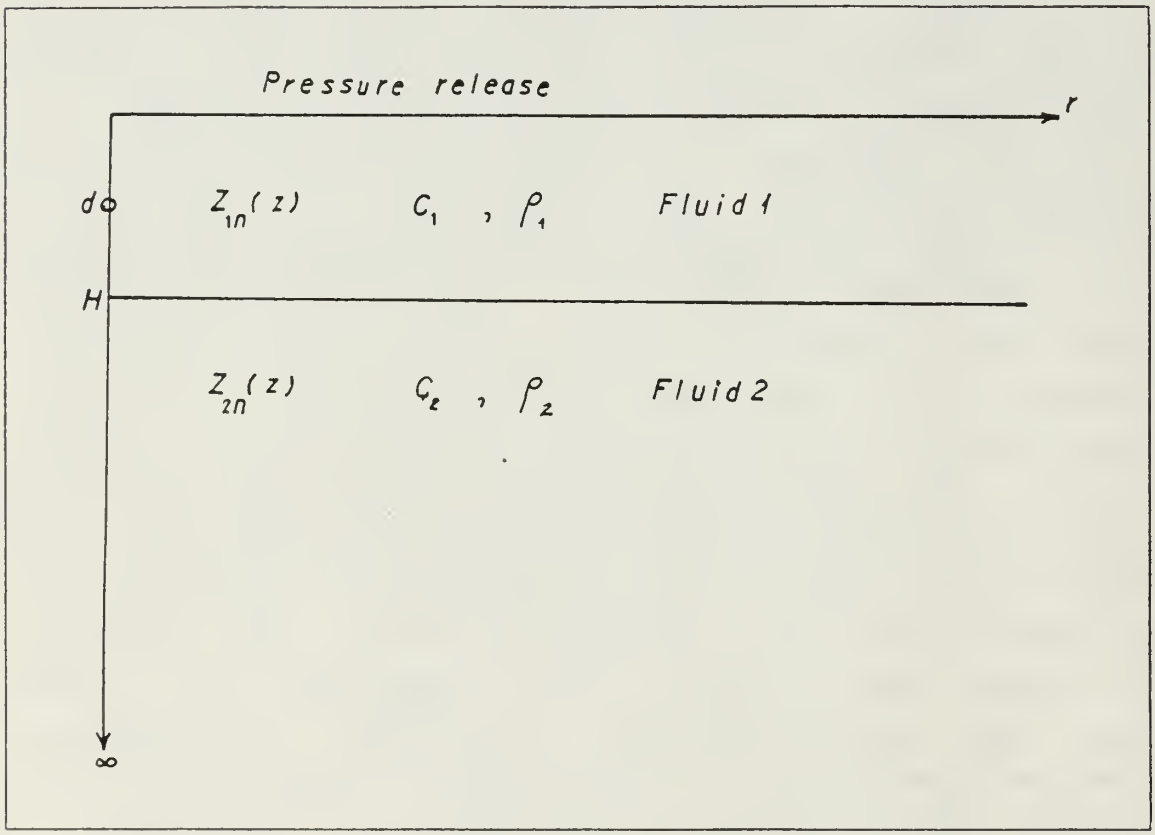

Figure 2.1 Two homogeneous layers with pressure release surface.

Let ρ_1, C_1 and ρ_2, C_2 be the constant densities and sound speeds in layer 1 and 2 respectively. Assume there is a point source at z = d in layer 1. The wave equation for a homogeneous medium can be written as ·

$$\nabla^2 \underset{\sim}{P} - \frac{1}{c^2}\frac{\partial^2 \underset{\sim}{P}}{\partial t^2} = -\sigma \qquad (2.1)$$

where σ is a source function and is defined by

$$\sigma = \frac{\partial Q}{\partial t}$$

Where Q is source strength

In our solution, we assume that a point source radiating a single frequency can be described mathematically by

$$\sigma = 4\pi A \delta(\underset{\sim}{r} - \underset{\sim}{r}_s) e^{j\omega t} \qquad (2.2)$$

Where $\delta(\underset{\sim}{r} - \underset{\sim}{r}_s)$ is the Dirac delta function, $\underset{\sim}{r}$ is the position vector. A is the amplitude factor which is assumed to be unity, and ω is the angular frequency of the source. Solution to the wave equation is of the form

$$\underset{\sim}{P}(\underset{\sim}{r}, t) = P(\underset{\sim}{r}) e^{j\omega t} \qquad (2.3)$$

Substituting equation (2.2) and equation (2.3) into equation (2.1) we get the helmholtz equation

$$\nabla^2 P + k^2 P = -4\pi \delta(\underset{\sim}{r} - \underset{\sim}{r}_s) \qquad (2.4)$$

where k is wave number defined by

$$k = \frac{\omega}{c} \tag{2.5}$$

The delta function for the point source at r = d is

$$\delta(\underset{\sim}{r} - \underset{\sim}{r}_s) = \frac{1}{2\pi r}\,\delta(r)\,\delta(z-d) \tag{2.6}$$

In cylindrical co-ordinates equation (2.4) can be written as

$$\left[\frac{1}{r}\frac{\partial}{\partial r}\left(r\frac{\partial}{\partial r}\right) + \frac{\partial^2}{\partial z^2} + k^2\right]\underset{\sim}{P} = -\frac{2}{r}\,\delta(r)\,\delta(z-d)\cdot e^{j\omega t} \tag{2.7}$$

This is an inhomogeneous equation. First, let us consider the homogeneous equation,

$$\left[\frac{1}{r}\frac{\partial}{\partial r}\left(r\frac{\partial}{\partial r}\right) + \frac{\partial^2}{\partial z^2} + k^2\right]\underset{\sim}{P} = 0 \tag{2.8}$$

and use the separation of variables technique.

We assume that the sound energy is trapped in the upper layer and solution to equation (2.8) can be represented by a set eigenfunctions.

$$\underset{\sim}{P}(r,z,t) = e^{j\omega t}\sum_n \underset{\sim n}{R}(r)\,Z_n(z) \tag{2.9}$$

Substitute equation (2.9) into equation (2.8) to get

$$\left[\sum_n Z_n \frac{1}{r} \frac{\partial}{\partial r}\left(r \frac{\partial \tilde{R}_n}{\partial r}\right) + \sum_n \tilde{R}_n \frac{\partial^2 Z}{\partial z^2} + \sum_n \tilde{R}_n Z_n k^2 \right] = 0 \quad (2.10)$$

or

$$\left[\frac{1}{\tilde{R}_n} \frac{1}{r} \frac{d}{dr}\left(r \frac{d \tilde{R}_n}{d r}\right)\right] + \left[\frac{1}{Z_n} \frac{d^2 Z_n}{d z^2} + k^2 \right] = 0 \quad (2.11)$$

This is only possible if each part in the square brackets in equation (2.11) is equal to a constant hence it can be written as

$$\frac{1}{\tilde{R}_n} \frac{1}{r} \frac{d}{dr}\left(r \frac{d \tilde{R}_n}{d r}\right) = - k_n^2 \quad (2.12)$$

$$\frac{1}{Z_n} \frac{d^2 Z_n}{dz^2} + k^2 = k_n^2 \quad (2.13)$$

where k_n is separation constant.

The boundary conditions on the depth functions are

$$Z_{1n}(0) = 0 \quad (2.14)$$

$$Z_{1n}(H) = Z_{2n}(H) \tag{2.15}$$

$$\frac{1}{\rho_1}\left(\frac{dZ_{1n}}{dz}\right)_H = \frac{1}{\rho_2}\left(\frac{dZ_{2n}}{dz}\right)_H \tag{2.16}$$

$$\lim_{z\to\infty} Z_{2n}(z) = 0 \tag{2.17}$$

Rewrite equation (2.13) in the form

$$\frac{d^2Z_n}{dz^2} + \left(k^2 - k_n^2\right)Z_n = 0$$

or

$$\frac{d^2Z_n}{dz^2} + k_{zn}^2 Z_n = 0 \tag{2.18}$$

where

$$k_{zn}^2 = \left(\frac{\omega}{c_1}\right)^2 - k_n^2 \tag{2.19}$$

In order to satisfy the boundary condition the pressure goes to zero when $Z \longrightarrow \infty$, the solution Z_{2n} must decay exponentially with depth. The only way that Z_{1n} can satisfy

the boundary conditions at the surface at Z = H is to be sinusoidal function of depth. Therefore

$$Z_{1n} = A_n \sin k_{zn} z \qquad 0 \le Z \le H \qquad (2.20)$$

$$Z_{2n} = B_n e^{-\beta_n z} \qquad H \le Z \le \infty \qquad (2.21)$$

$$\beta_n^2 = k_n^2 - \left(\frac{\omega}{C_2}\right)^2 \qquad (2.22)$$

Waveguide propagation requires that k_n and β_n must be real hence

$$\frac{\omega}{C_2} \le k_n \le \frac{\omega}{C_1} \qquad (2.23)$$

Application of boundary Conditions at Z = H results in

$$A_n \sin k_{zn} H = B_n e^{-\beta_n H} \qquad (2.24)$$

$$A_n \frac{1}{\rho_1} k_{zn} \cos k_{zn} H = -\frac{1}{\rho_2} \beta_n B_n e^{-\beta_n H} \qquad (2.25)$$

which gives

$$B_n = A_n e^{\beta_n H} \cdot \sin k_{zn} H \tag{2.26}$$

The depth function, therefore, can now be written as

$$Z_{1n}(z) = A_n \sin k_{zn} z \qquad 0 \le z \le H \tag{2.27}$$

$$Z_{2n}(z) = A_n \sin k_{zn} H \cdot e^{-\beta_n (z-H)} \qquad H \le z \le \infty \tag{2.28}$$

These depth functions have to be orthogonal. Since there is a discontinuity in the slope at the boundary Z = H, we need separate orthogonality constant for each layer. We assume that the constant is unity for the layer 1 and γ for the layer 2.

$$Z_n(z) = \begin{cases} Z_{1n}(z) & 0 \le z \le H \\ \gamma Z_{2n}(z) & H \le z \le \infty \end{cases} \tag{2.29}$$

In order to evaluate γ multiply equation (2.13) by Z_m

$$Z_m \frac{d^2 Z}{dz^2} + (k^2 - k_n^2) Z_n Z_m = 0 \tag{2.30}$$

interchange the subscript m and n in equation (2.30) and take the difference of the two equations to get

$$\frac{d}{dz}\left(Z_m \frac{dZ_n}{dz} - Z_n \frac{dZ_m}{dz}\right) = \left(k_n^2 - k_m^2\right) Z_m Z_n \qquad (2.31)$$

Integrate both sides of equation (2.31) from 0 to ∞

$$\int_0^\infty \frac{d}{dz}\left(Z_m \frac{dZ_n}{dz} - Z_n \frac{dZ_m}{dz}\right) dz = \left(k_n^2 - k_m^2\right) \int_0^\infty Z_m Z_n dz \qquad (2.32)$$

The orthogonality condition requires that, for $m \neq n$, the R.H.S of the equation (2.32) must be zero. Therefore

$$\int_0^H \frac{d}{dz}\left(Z_{1m} \frac{dZ_{1n}}{dz} - Z_{1n} \frac{dZ_{1m}}{dz}\right) dz + \gamma^2 \int_H^\infty \frac{d}{dz}\left(Z_{2m} \frac{dZ_{2n}}{dz} - Z_{2n} \frac{dZ_{2m}}{dz}\right) dz = 0 \qquad (2.33)$$

$$\left[Z_{1m} \frac{dZ_{1n}}{dz} - Z_{1n} \frac{dZ_{1m}}{dz}\right]_0^H + \gamma^2 \left[Z_{2m} \frac{dZ_{2n}}{dz} - Z_{2n} \frac{dZ_{2m}}{dz}\right]_H^\infty = 0 \qquad (2.34)$$

The application of limits as well as boundary conditions gives

$$\left[1 - \gamma^2 \frac{\rho_2}{\rho_1}\right]\left[Z_{1m}(H)\left(\frac{dZ_{1n}}{dz}\right)_H - Z_{1n}(H)\left(\frac{dZ_{1m}}{dz}\right)_H\right] = 0 \qquad (2.35)$$

This is only possible if

$$1 - \gamma^2 \frac{\rho_2}{\rho_1} = 0$$

or

$$\gamma = \sqrt{\frac{\rho_1}{\rho_2}} \qquad (2.36)$$

Therefore, equation (2.29) becomes

$$Z_n = \begin{cases} A_n Z_{1n}(z) & 0 \le z \le H \\ \sqrt{\frac{\rho_1}{\rho_2}}\, A_n Z_{2n}(z) & H \le z \le \infty \end{cases} \qquad (2.37)$$

We will normalize the depth eigenfunctions in order to evaluate A_n , consider the m = n case

$$\int_0^\infty Z_n^2(z)\,dz = 1 \qquad (2.38)$$

$$\int_0^H A_n^2 Z_{1n} Z_{1n}\,dz + \int_H^\infty \frac{\rho_1}{\rho_2} A_n^2 Z_{2n} Z_{2n}\,dz = 1 \qquad (2.39)$$

$$A_n^2 = \frac{1}{\int_0^H Z_{1n}^2\,dz + \frac{\rho_1}{\rho_2}\int_H^\infty Z_{2n}^2\,dz} \qquad (2.40)$$

Now

$$\int_0^H Z_{1n}^2 dz = \int_0^H \frac{1}{2}(1 - \cos 2k_{zn} z)dz \qquad (2.41)$$

Integrating and substituting the limit we get

$$\int_0^H Z_{1n}^2 dz = \frac{1}{2}\left[H - \frac{1}{k_{zn}} \sin k_{zn} H \cdot \cos k_{zn} H\right] \qquad (2.42)$$

and

$$\int_H^\infty Z_{2n}^2 dz = \int_H^\infty (\sin^2 k_{zn} H \cdot e^{2\beta_n H}) \cdot e^{-2\beta_n z} dz \qquad (2.43)$$

or

$$\int_H^\infty Z_{2n}^2 dz = \frac{1}{2\beta_n} \sin^2 k_{zn} H \qquad (2.44)$$

Substituting equation (2.42) and equation (2.44) into equation (2.40) gives

$$A_n^2 = \frac{2 \cdot k_{zn}}{k_{zn} H - \cos(k_{zn} H)\sin(k_{zn} H) - \left(\frac{\rho_1}{\rho_2}\right)^2 \sin^2(k_{zn} H) \cdot \tan(k_{zn} H)} \qquad (2.45)$$

The depth eigenfunctions now form a complete set of orthonormal functions.

Now we have to evaluate the Green's function for the inhomogeneous wave equation

$$\sum_n Z_n \frac{1}{r}\frac{\partial}{\partial r}\left(r\frac{\partial \tilde{R}_n}{\partial r}\right)+\sum_n \tilde{R}_n \frac{\partial^2 Z_n}{\partial z^2}+\sum_n \tilde{R}_n Z_n\left(\frac{\omega}{c}\right)^2=-\frac{2}{r}\delta(r)\,\delta(z-d) \tag{2.46}$$

$$\sum_n Z_n\left[\frac{1}{r}\frac{d}{dr}\left(r\frac{d\tilde{R}_n}{dr}\right)+k_n^2\tilde{R}_n\right]+\sum_n \tilde{R}_n\left[\frac{d^2 Z_n}{dz^2}+\left(k^2-k_n^2\right)Z_n\right]=-\frac{2}{r}\delta(r)\,\delta(z-d) \tag{2.47}$$

From equation (2.13), the second term in the square bracket is zero; therefore, equation (2.47) can be rewritten as

$$\sum_n Z_n\left[\frac{1}{r}\frac{d}{dr}\left(r\frac{d\tilde{R}_n}{dr}\right)+k_n\tilde{R}_n\right] = -\frac{2}{r}\delta(r)\,\delta(z-d) \tag{2.48}$$

Multiply both sides of equation (2.48) by Z_m and integrate from 0 to ∞ gives

$$\sum_n\left[\frac{1}{r}\frac{d}{dr}\left(r\frac{d\tilde{R}_n}{dr}\right)+k_n^2\tilde{R}_n\right]\int_0^\infty Z_m Z_n\,dz = -\frac{2}{r}\delta(r)\int_0^\infty \delta(z-d)\,Z_m\,dz \tag{2.49}$$

For m = n

$$\frac{1}{r}\frac{d}{dr}\left(r\frac{d\tilde{R}_n}{dr}\right)+k_n^2\tilde{R}_n = -\frac{2}{r}\delta(r)Z_n(d) \tag{2.50}$$

Solution to this homogeneous equation is

$$\underset{\sim}{R}_n(r) = -j\pi Z_n(d) H_0^{(2)}(k_n r) \qquad (2.51)$$

where for $k_n r >> 1$

$$H_o^{(2)}(k_n r) \approx \sqrt{\frac{2}{\pi k_n r}} \cdot e^{-j(k_n r - \frac{\pi}{4})}$$

The Hankel function $H_o^{(2)}(k_n r)$ describes the solution in the r direction.

Therefore, the solution for the sound trapped in layer 1 ($0 \leq Z \leq H$) is

$$\underset{\sim}{P}(r,z,t) = -j \sum_n \sqrt{\frac{2\pi}{k_n r}} A_n^2 \sin(k_{zn} d) \sin(k_{zn} z) e^{j(\omega t - k_n r + \frac{\pi}{4})} \qquad (2.52)$$

Equation (2.52) is invariant under the interchange of Z and d and is valid within the region $0 \leq Z \leq H$. The eigenvalues k_{zn} can be obtained by eliminating B_n from equation (2.25)

$$\tan k_{zn} H = -\frac{\rho_2}{\rho_1} \frac{k_{zn}}{\beta_n} \qquad (2.53)$$

Let

$$X_n = k_{zn} H \quad ; \quad b = \frac{\rho_1}{\rho_2} \qquad (2.54)$$

$$\tan X_n = \frac{-X_n}{bH\sqrt{k_n^2 - \left(\frac{\omega}{c_2}\right)^2}} \qquad (2.55)$$

$$\frac{\tan X_n}{X_n} = \frac{-1}{bH\sqrt{\frac{\omega^2}{c_1^2} - \frac{\omega^2}{c_2^2} - \frac{X_n^2}{H^2}}} \qquad (2.56)$$

When $C_2 > C_1$ which is the case under consideration, equation (2.56) possesses real roots for k_n and X_n, the later varying in the range $(n - 1/2)\pi \leq X_n \leq n\pi$. On the other hand, when $C_2 < C_1$, the roots k_n are complex numbers with negative imaginary parts. In the later case, therefore, the factor $\exp(-jk_n r)$ in equation (2.52) implies horizontal attenuation. In the case of a fast bottom, there exist solutions which suffer no horizontal damping. This condition stems, of course, from the fact that for angles of incidence (measured from the normal) greater than critical angle, no power is transmitted into the bottom. Figures 2.2, 2.3, and 2.4 shows the z dependence of the first three normal modes for 50 kHz, 120 kHz, 160 kHz respectively. Figure 2.5 shows the r dependence of the sound pressure.

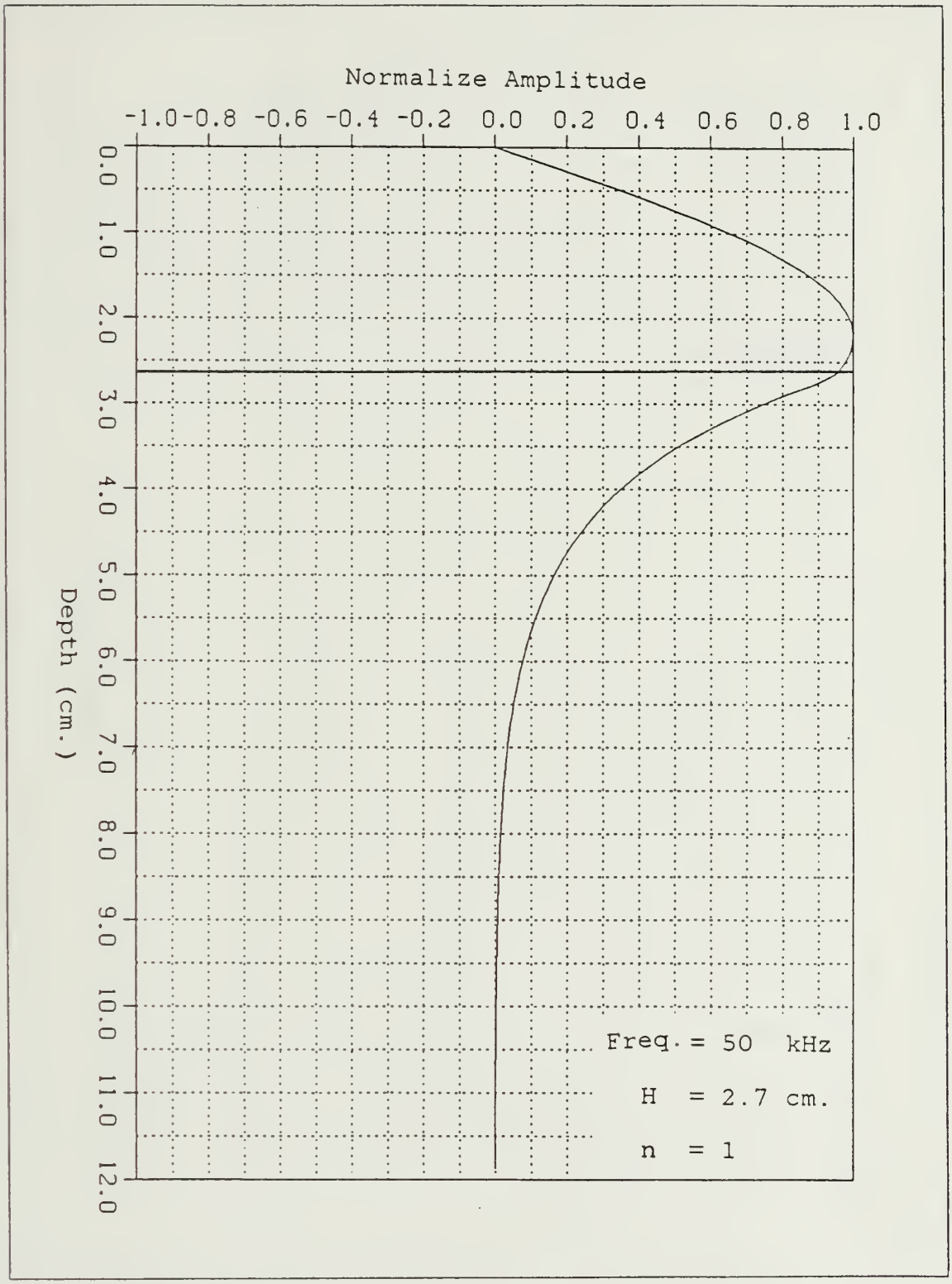

Figure 2.2 Pressure amplitude vs depth for first mode.

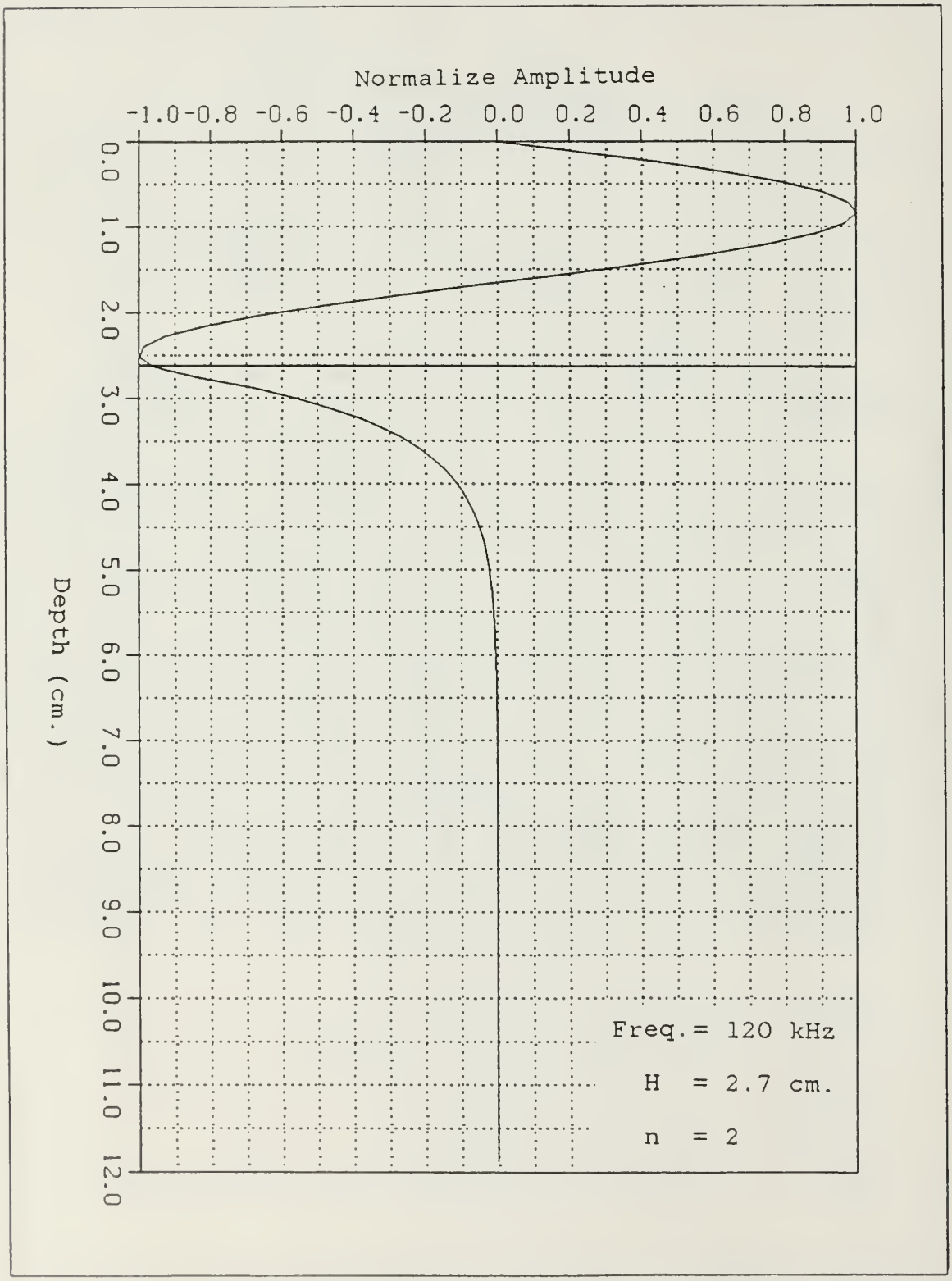

Figure 2.3 Pressure amplitude vs depth for second mode.

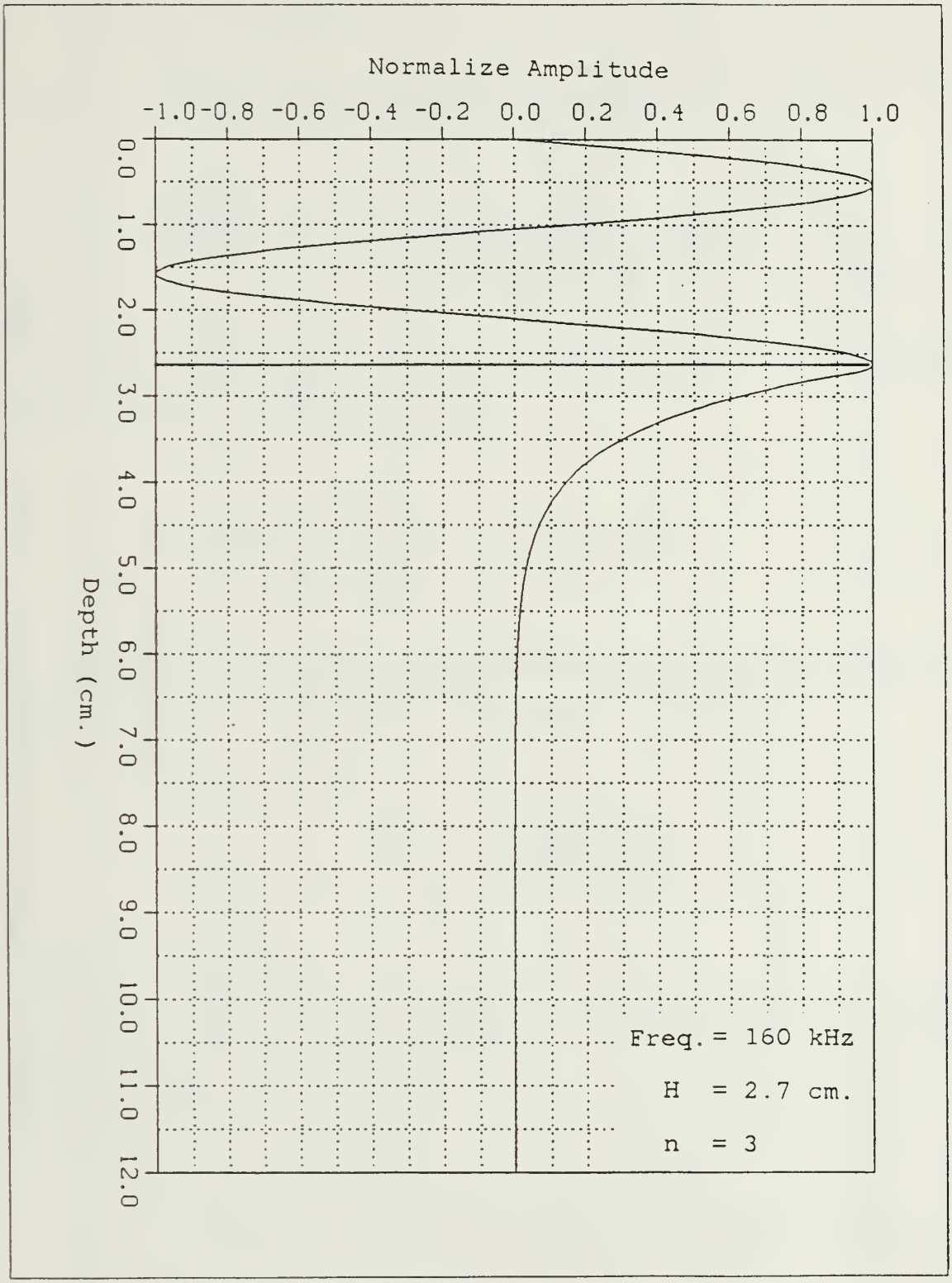

Figure 2.4 Pressure amplitude vs depth for third mode.

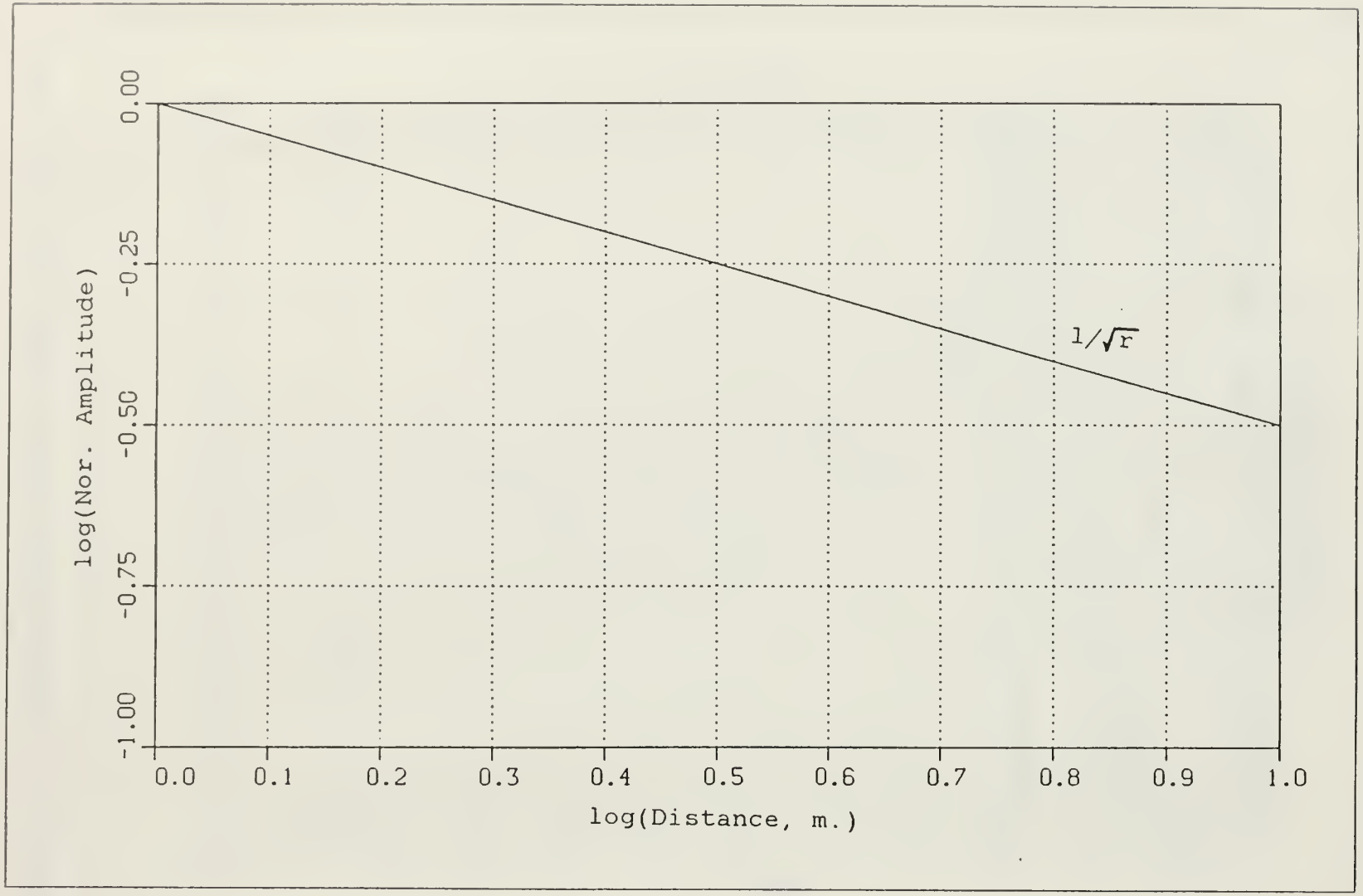

Figure 2.5 Pressure amplitude as a function of range.

C. CUT - OFF FREQUENCY

Let us determine the cut-off frequencies of the normal modes. It follows from equation (2.56) that

$$\frac{\tan X_n}{X_n} = \frac{-1}{b\sqrt{\omega^2 H^2\left(\frac{1}{C_1^2}-\frac{1}{C_2^2}\right)-X_n^2}} \qquad (2.57)$$

It is clear from the above equation that the nth mode cannot support propagation until

$$\omega^2 H^2\left(\frac{1}{C_1^2}-\frac{1}{C_2^2}\right) \geq \left[\left(n-\frac{1}{2}\right)\pi\right]^2 \qquad (2.58)$$

Therefore, the limiting frequency below which transmission of the nth mode cannot take place is given by

$$f_n = \frac{(2n-1)C_1}{4H\sqrt{1-\frac{C_1^2}{C_2^2}}} \qquad (2.59)$$

where n = 1,2,3,-----

This is an important relation between the layer thickness H and the cut-off frequency f_n . It is shown in Figure 2.6 for the first mode.

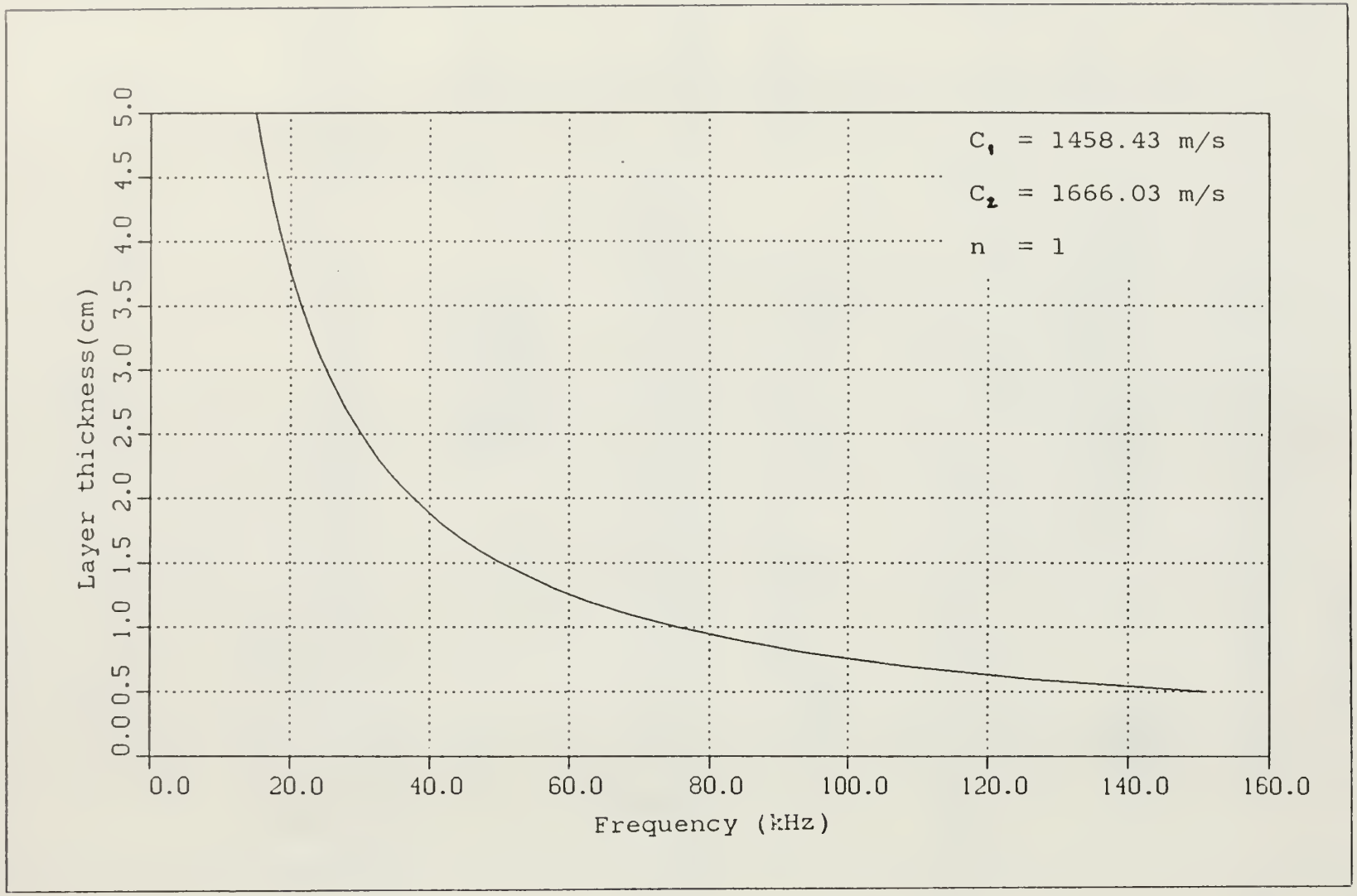

Figure 2.6 Cut-off frequency as function of layer thickness.

D. PHASE SPEED

The factor exp $j(\omega t - k_n r + \pi/4)$ in equation (2.52) allows an obvious interpretation of k_n, namely $k_n = \omega/Cpn$ where C_{pn} is the phase speed of the nth mode. The phase speed is the speed that the wave front (surface of constant phase) propagates in r direction. The phase speed at the cut-off frequency has the value of the speed of sound in the bottom and decreases continuously with the increasing frequency towards the value of sound speed in the upper layer. From equation (2.19) we can write [Ref. 3]

$$k_n^2 = \left(\frac{\omega}{C_1}\right)^2 - k_{zn}^2 \qquad (2.60)$$

Multiply both sides by H^2 gives

$$k_n^2 H^2 = \left(\frac{\omega H}{C_1}\right)^2 - k_{zn}^2 H^2 \qquad (2.61)$$

or

$$\omega^2 H^2 = C_1^2 (k_n^2 H^2 + k_{zn}^2 H^2)$$

or

$$\omega^2 H^2 = C_1^2 (\alpha_n^2 + X_n^2) \qquad (2.62)$$

where

$$\alpha_n^2 = k_n^2 H^2 \tag{2.63}$$

Therefore equation (2.57) can be written as

$$\frac{\tan X_n}{X_n} = \frac{-1/b}{H\sqrt{\left(\frac{\alpha_n}{H}\right)^2 - \left(\frac{\omega}{c_2}\right)^2}} \tag{2.64}$$

or

$$\frac{\tan X_n}{X_n} = \frac{-\delta}{\sqrt{\alpha_n^2 \epsilon^2 - X_n^2}} \tag{2.65}$$

where

$$\delta = \frac{\rho_2 c_2}{\rho_1 c_1} \tag{2.66}$$

$$\epsilon^2 = \left(\frac{c_2}{c_1}\right)^2 - 1 \tag{2.67}$$

From equation (2.65)

$$\alpha_n = \frac{X_n}{\epsilon}\sqrt{1 + \delta^2 \cot^2(X_n)} \tag{2.68}$$

We know that $\alpha_n = k_n H$ where $k_n = \omega/C_{pn}$.
C_{pn} is the phase speed of the nth mode.
Therefore

$$C_{pn} = \frac{\omega \cdot H}{\alpha_n} \qquad (2.69)$$

From equation (2.62) we have

$$\omega \cdot H = C_1 \sqrt{\alpha_n^2 + X_n^2} \qquad (2.70)$$

Hence

$$C_{pn} = C_1 \sqrt{1 + \left(\frac{X_n}{\alpha_n}\right)^2} \qquad (2.71)$$

Substituting the value of X_n/α_n from equation (2.68) we get

$$C_{pn} = C_1 \cdot \left[1 + \frac{\epsilon^2}{1 + \delta^2 \cot^2(X_n)}\right]^{\frac{1}{2}} \qquad (2.72)$$

$(n-1/2)\pi \leq X_n \leq n\pi$ for the nth mode, and in this case k_n and phase speed are real and propagation of the modes proceed without damping. X_n is a function of angular frequency and the frequency corresponding to any given value of X_n can be obtained.

$$\gamma \equiv \frac{\omega H}{2\pi c_1} = \frac{H}{\lambda} = \frac{\alpha_n c_{pn}}{2\pi c_1}$$

$$= \frac{X_n}{2\pi\epsilon}\sqrt{1+\epsilon^2+\delta^2\cot^2 X_n} \qquad (2.73)$$

When X_n is near its upper limit of $n\pi$, then cot $X \to \infty$. Therefore γ is very large and from equation (2.72)

$$c_{pn} \longrightarrow c_1$$

Hence in the limit of very high frequency, phase speed approaches the sound speed c_1. When X_n is near its lower limits $(n-1/2)\pi$ then cot $X \to 0$.

and $$c_{pn} = c_1\left[1+\epsilon^2\right]^{\frac{1}{2}} = c_2$$

The phase speed, therefore, varies from the value c_2 at the critical frequency down to c_1 in the limit of very high frequency. Figure (2.7) shows the phase speed as a function of frequency for first three modes.

E. GROUP SPEED

In a medium in which the phase speed varies with frequency and if the pressure pulse from a point source is not a single frequency but covers a moderately broad spectrum, then the presence of the particular frequency component of the spectrum at a large range would occur at a time associated with the group speed (speed with which the energy associated with a particular frequency will travel). At frequencies ω for which the phase is stationary, mutual interference will be negligible and these

frequencies will be dominant at the prescribed values of t and r. The values of t and r for which the phase is stationary for a given frequency, therefore, determine the rate of propagation of this frequency in the mutually interfering train of sinusoidal waves, [Ref. 3], called group speed C_g .

$$f(\omega, r, t) = \omega t - k_n(\omega) r + \frac{\pi}{4} \tag{2.74}$$

$$\frac{df}{d\omega} = t - r\frac{dk_n}{d\omega} = 0 \tag{2.75}$$

$$C_{gn} = \frac{r}{t} = \frac{d\omega}{dk_n} \tag{2.76}$$

but

$$\omega = k_n C_{pn}$$

Therefore

$$C_{gn} = \frac{d\omega}{dk_n} = \frac{d(k_n C_{pn})}{dk_n} = C_{pn} + k_n \frac{dC_{pn}}{dk_n} \tag{2.77}$$

From equation (2.63) we have $k_n = \alpha_n/H$. Substituting this value in equation (2.77), we get

$$C_{gn} = C_{pn} + \alpha_n \frac{dC_{pn}}{d\alpha_n} \tag{2.78}$$

From equation (2.71) we can write

$$\frac{dC_{pn}}{d\alpha_n} = \frac{C_1}{2}\left[1 + \left(\frac{X_n}{\alpha_n}\right)^2\right]^{-\frac{1}{2}} \cdot 2\left[\frac{X_n}{\alpha_n}\right]\left[\frac{1}{\alpha_n}\frac{dX_n}{d\alpha_n} - \frac{X_n}{\alpha_n^2}\right]$$

$$\alpha_n \frac{dC_{pn}}{d\alpha_n} = \frac{C_1 X_n\left(\frac{dX_n}{d\alpha_n} - \frac{X_n}{\alpha_n}\right)}{\sqrt{\alpha_n^2 + X_n^2}} \tag{2.79}$$

From equation (2.68) we get

$$\frac{dX_n}{d\alpha_n} = \frac{\epsilon\sqrt{1 + \delta^2 \cot^2 X_n}}{\phi(X_n)} \tag{2.80}$$

And then substitution of equation (2.80) and equation (2.79) into equation (2.78) yields

$$\frac{C_{gn}}{C_1} = \left(\frac{C_1}{C_{pn}}\right)\left[1 + \frac{\epsilon^2}{\phi(X_n)}\right] \tag{2.81}$$

where

$$\phi(X_n) = \left[1 + \delta^2 \cot^2 X_n - \delta^2 X_n \cdot \cos X_n / \sin^3 X_n\right] \tag{2.82}$$

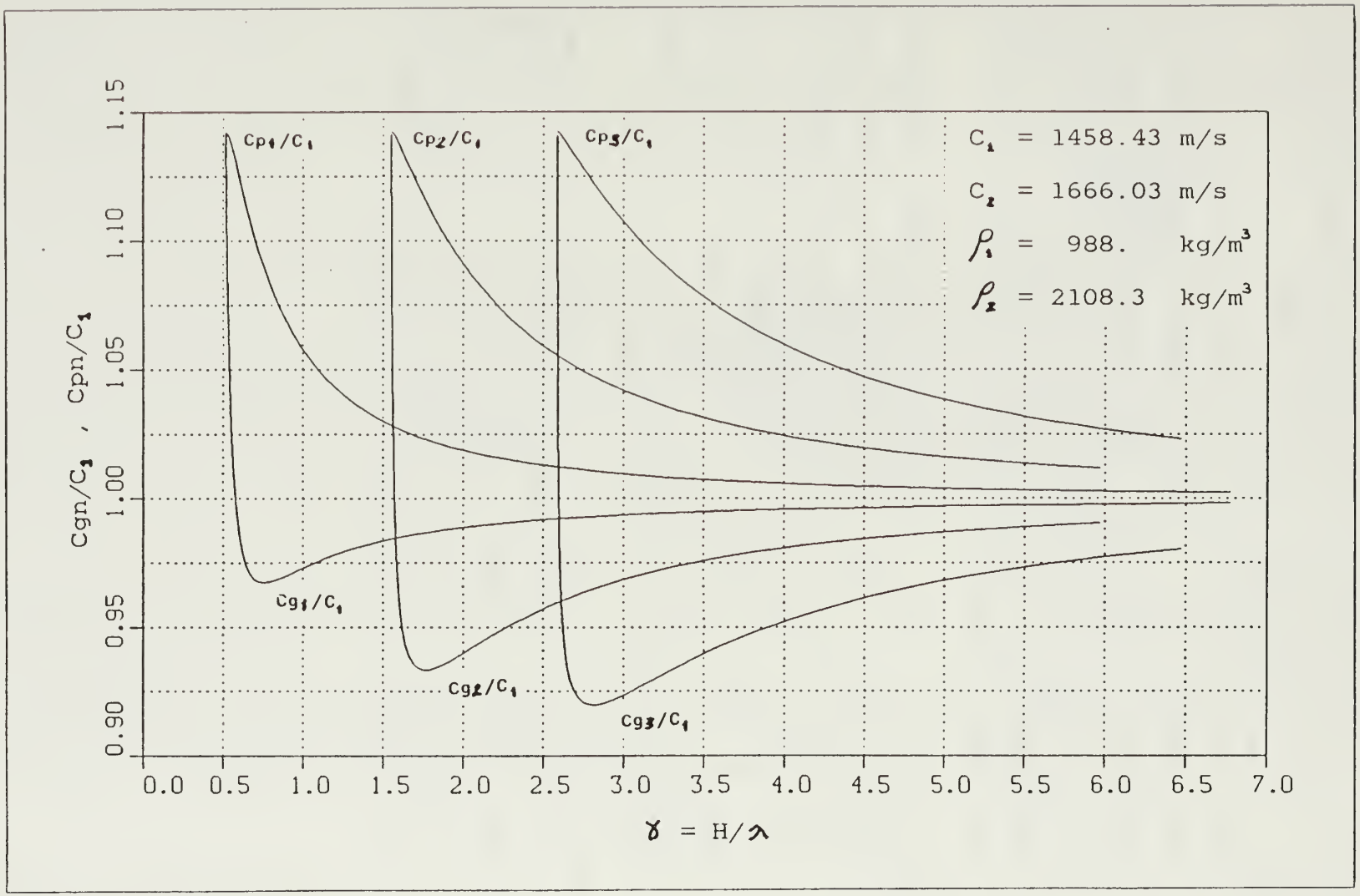

Figure 2.7 Group and phase speed as function of frequency.

Figure (2.7) shows the group speed as a function of frequency for first three modes. It may be noted that group speed is always less than the phase speed. The general features for each mode are, [Ref. 2].

1. The first arrival would be nearly sinusoidal waves of frequency f_n, where f_n denotes the limiting frequency for the n th mode. The wave would arrive at $t = r/C_2$ travelling with $C_{gn} = C_2$. This portion of the signal is called ground wave. As the time progresses, the frequency and amplitude in the ground wave would increase.

2. At time $t = r/C_1$ a new train of high frequency waves, due to the right hand branch of the group velocity curve, would suddenly be superimposed on the ground wave travelling with speed $C_{gn} = C_1$. This new high frequency wave is designated as water wave. The frequency in the water wave would decrease as time progresses while in the ground wave the frequency would continue to increase.

3. Still later f_g and f_w would approach each other at $t=r/C_{go}$, where C_{go} denote the minimum group speed they would coincide. The pressure then would consists of a single frequency f_A and this portion of the signal is called Airy phase. The sequence of these events is illustrated in Figure 2.8 .

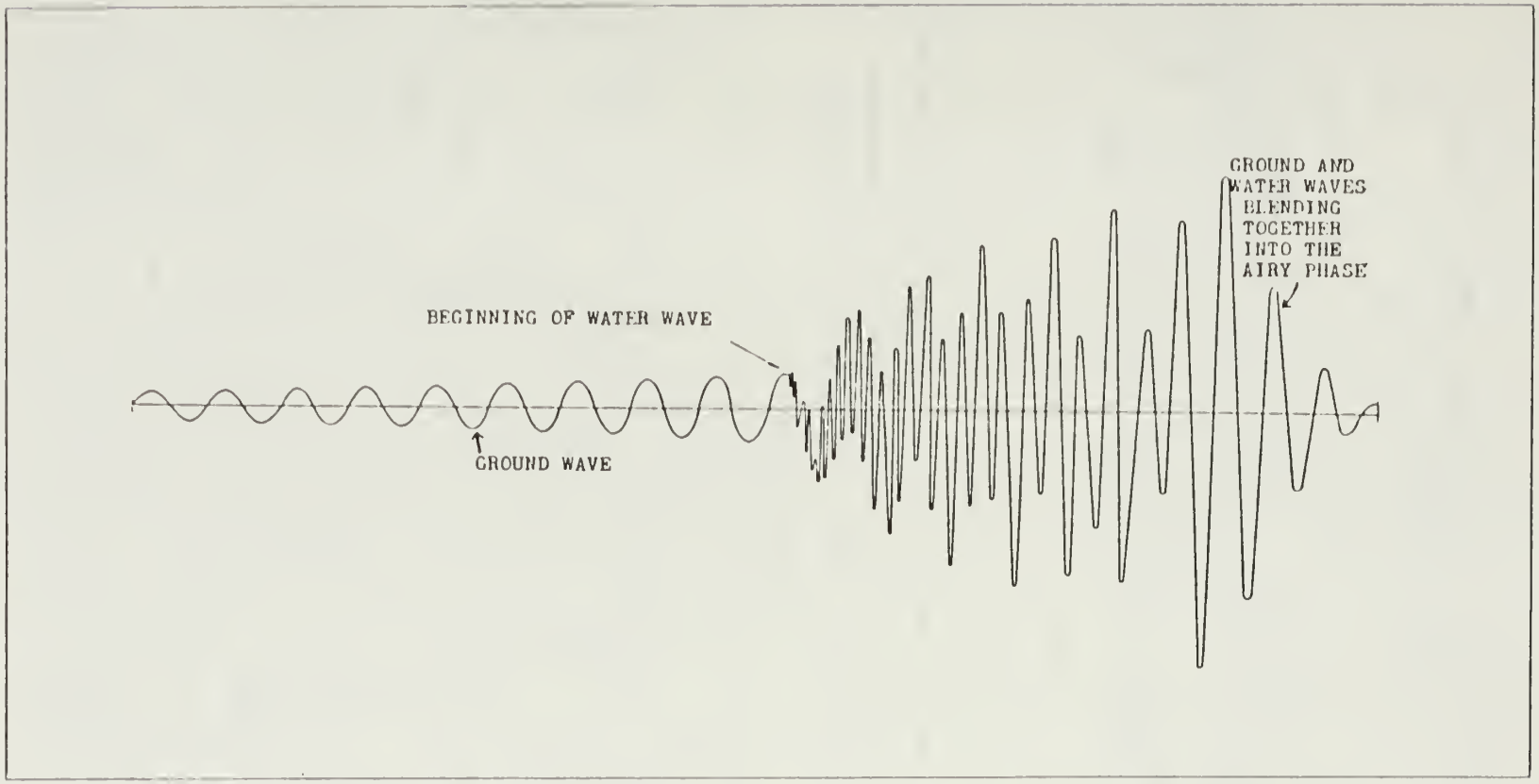

Figure 2.8 Received pressure transient in shallow water (Ref.3).

III. SOUND PROPAGATION IN A MODELED SHALLOW WATER ENVIRONMENT

A. INTRODUCTION

The purpose of this experiment was to investigate experimentally the behaviour of sound propagation in a laboratory facility consisting of a layer of water overlaying a layer of sand and to compare the results with the normal mode theory.

B. EQUIPMENT

1. The tank used for experimental work is made of aluminium plate one centimeter thick. The interior dimensions of the tank are :

Length	=	9.95 meters
Width	=	0.94 meters
Depth	=	0.24 meters

The tank has a carriage which can be used to adjust horizontal and vertical positions of receiver. The rails on which the carriage moves were leveled to ensure that receiver remained at a constant depth as it moved along the tank. The leveling arrangement was not precise and it was found that the total vertical variation of the receiver was within $\pm$ 1 mm. All the joints of the tank were sealed with silicon sealer and the interior of the tank was coated with three layers of primer paint (zinc chromate) to avoid corrosion. Wooden wedges are fixed on the inner sides of the tank to minimize the reflection of sound. The tank was filled with water saturated sand to form an 11 cm thick bottom layer and a thin layer of water (2 to 3 cm) was added above the sand. The sand was degassed by circulating water

deep into the sand with a centrifugal pump at moderate pressure. This process was repeated several times. The top surface of the sand was leveled with reference to the water surface. This leveled surface of sand was horizonally flat within ± 1 mm. The layer of water was very shallow and the thickness of this layer changes with time due to evaporation of the water. To avoid this, the tank was equiped with an automatic water level control which maintains the desired level of water.

2. The frequencies used in this work ranged from 25 kHz to 100 kHz. The source transducer was built from a rectangular crystal of piezoelectric material 2.98 cm long and 1.12 cm wide. The directivity index of the transducer at 50 kHz is 5.75 dB. The receiver was made from a 4 mm by 4 mm piezoceramic cylinder.

C. MEASUREMENT OF SPEED OF SOUND AND DENSITY

Figure 3.1 shows the equipment and the circuit used to measure the speed of sound in water-saturated sand and in water. Two LC-5 transducers were used as source and receiver. A high frequency tone burst of the order of one MHz was used and the speed of sound was calculated by direct measurement of time-of-flight from the oscilloscope and the distance between the source and the receiver. Experimentally determined values for the speed of sound in the sand and in water are shown in Table I and Table II. The standard deviation of the measurements is an indication of the precision of the measurement (approximately 1 percent). The difference between the measured speed of sound in water and the value predicted by theory at that temperature is an indication of the accuracy of the measurement (approximately 0.95 percent). The density of the sand was measured by weighing 1000 cm^3 of water-saturated sand and calculating its mass The measured values are shown in Table I.

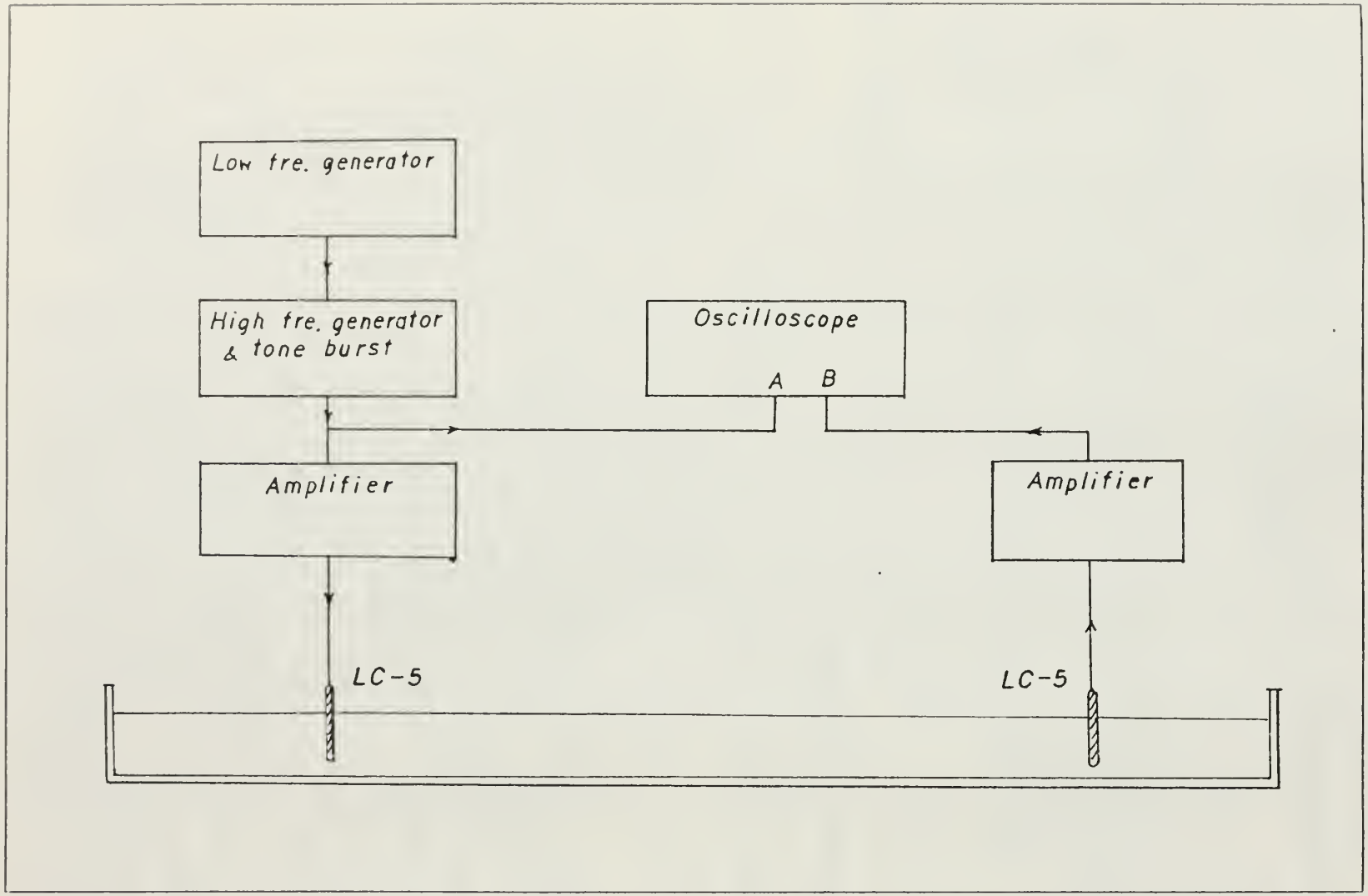

Figure 3.1 Measurement of speed of sound using 1 MHz tone burst.

TABLE I

Speed of sound in sand

No.	Time Division	Scale (μs/div)	Distance (cm)	C (m/s)
1	8.1	50	67.8	1674.07
2	6.4	50	54.3	1696.88
3	5.5	50	45.3	1647.27
4	4.6	50	38.0	1652.17
5	6.3	20	21.1	1674.6
6	8.6	10	14.2	1651.16

Average Speed = 1666.03 m/s

Standard Deviation = 17.58

Percent Deviation = 1.06 %

Measurement For Density of Sand

Mass of the Container = 542 gm

Mass of 1000 cm^3 of sand + Container = 2650.3 gm

Density = 2108.3 kg/m^3

TABLE II

Speed of sound in water (Temperature = 17° C)

No.	Time Division	Scale (μs/div)	Distance (cm)	C (m/s)
1	3.8	50	27.5	1447.3
2	4.5	50	33.0	1466.67
3	6.0	50	43.5	1450.0
4	7.05	50	51.5	1461.0
5	8.8	50	64.5	1465.91
6	5.0	100	72.2	1444.0
7	5.7	100	83.7	1468.42
8	6.4	100	93.7	1464.06

Average Speed of Sound = 1458.43 m/s

Standard Deviation = 9.1

Speed of Sound from Theory = 1472.39 m/s

Percent Deviation = 0.95 %

D. VOLTAGE RESPONSE AND SENSITIVITY OF TRANSDUCERS

The basic characteristics of the source and receiver were not known, therefore the voltage response of the transmitter and the sensitivity of the receiver were measured by the reciprocity method (Figure 3.2). The left hand side of the Figure indicates the transducers being used as transmitters and the right hand side as receivers. Experimentally measured data are shown in Table III and calculated values of voltage response and sensitivity are shown in Table IV. The voltage response of the transmitter is plotted in Figure 3.3 and sensitivity of the receiver in Figure 3.4 .

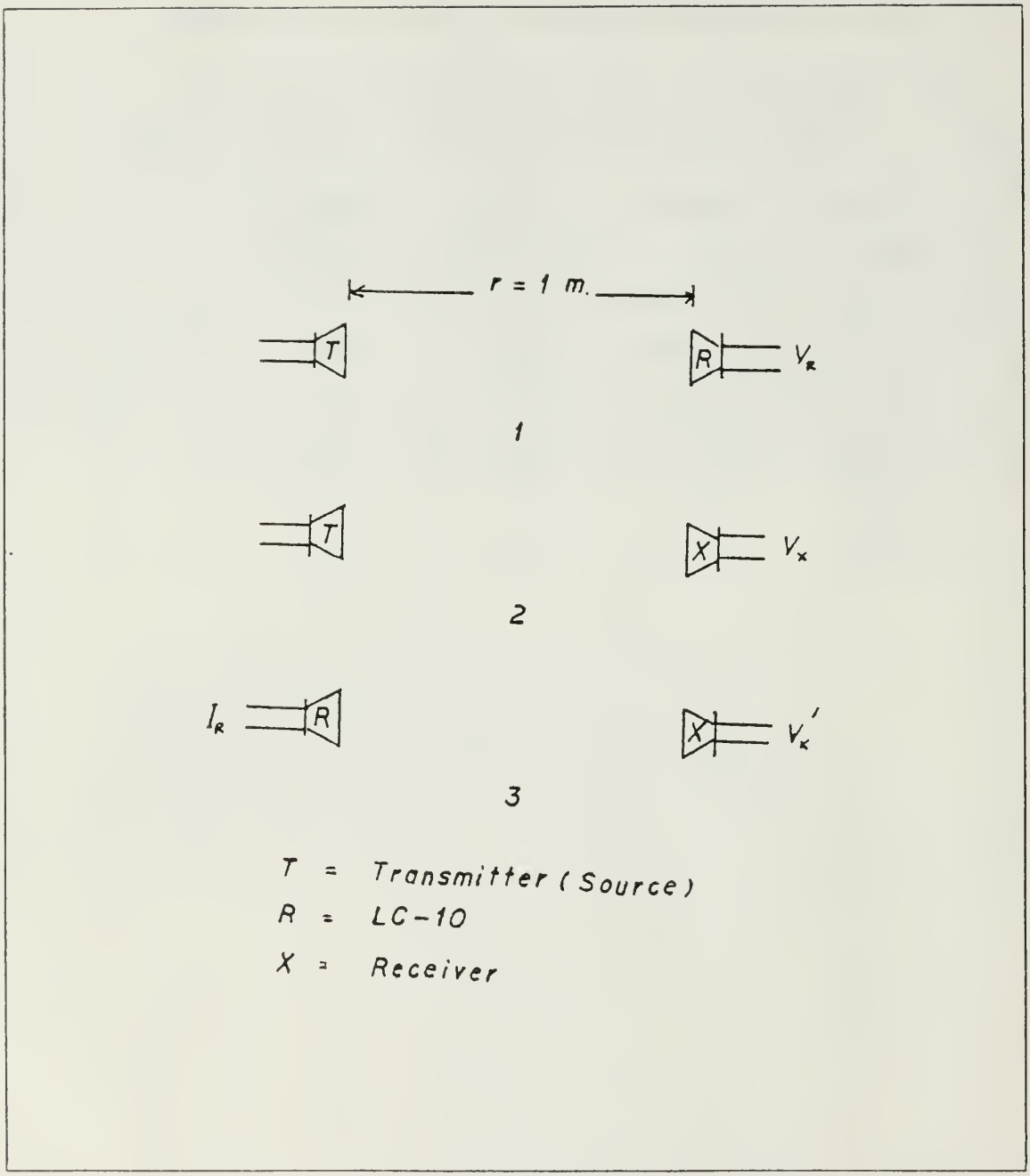

Figure 3.2 Calibration of transducers by reciprocity method.

TABLE III

Experimental measurements for calibrations of transducers

Fre. (kHz)	V_R (volt)	V_x (volt)	I_R (amp)	V_x' (volt)
20	0.00046	0.0015	0.0051	0.00036
30	0.00073	0.002	0.0075	0.006
40	0.0012	0.0016	0.01	0.012
50	0.00175	0.0074	0.0127	0.034
60	0.00255	0.0071	0.0155	0.044
70	0.003	0.0227	0.0185	0.099
80	0.0046	0.018	0.0215	0.224
90	0.006	0.059	0.025	0.46
100	0.0075	0.0625	0.0275	0.62
110	0.01	0.185	0.0305	1.15
120	0.0123	0.089	0.0315	0.17
130	0.016	0.085	0.034	0.193
140	0.015	0.06	0.037	0.1
150	0.0145	0.093	0.043	0.21

Distance between source and receiver = 1 m.

Applied voltage = 5 volts

TABLE IV

Voltage response and sensitivity

Fre. (kHz)	Sensitivity dB(re V/Pa)	Voltage Response dB(re Pa/V @ 1 m)
20	-76.37	5.91
30	-68.34	0.38
40	-70.96	1.06
50	-63.43	6.84
60	-65.78	8.83
70	-59.36	12.50
80	-59.91	11.03
90	-53.95	15.39
100	-54.24	16.18
110	-48.96	20.32
120	-61.86	26.87
130	-63.33	27.94
140	-68.10	29.69
150	-63.68	29.07

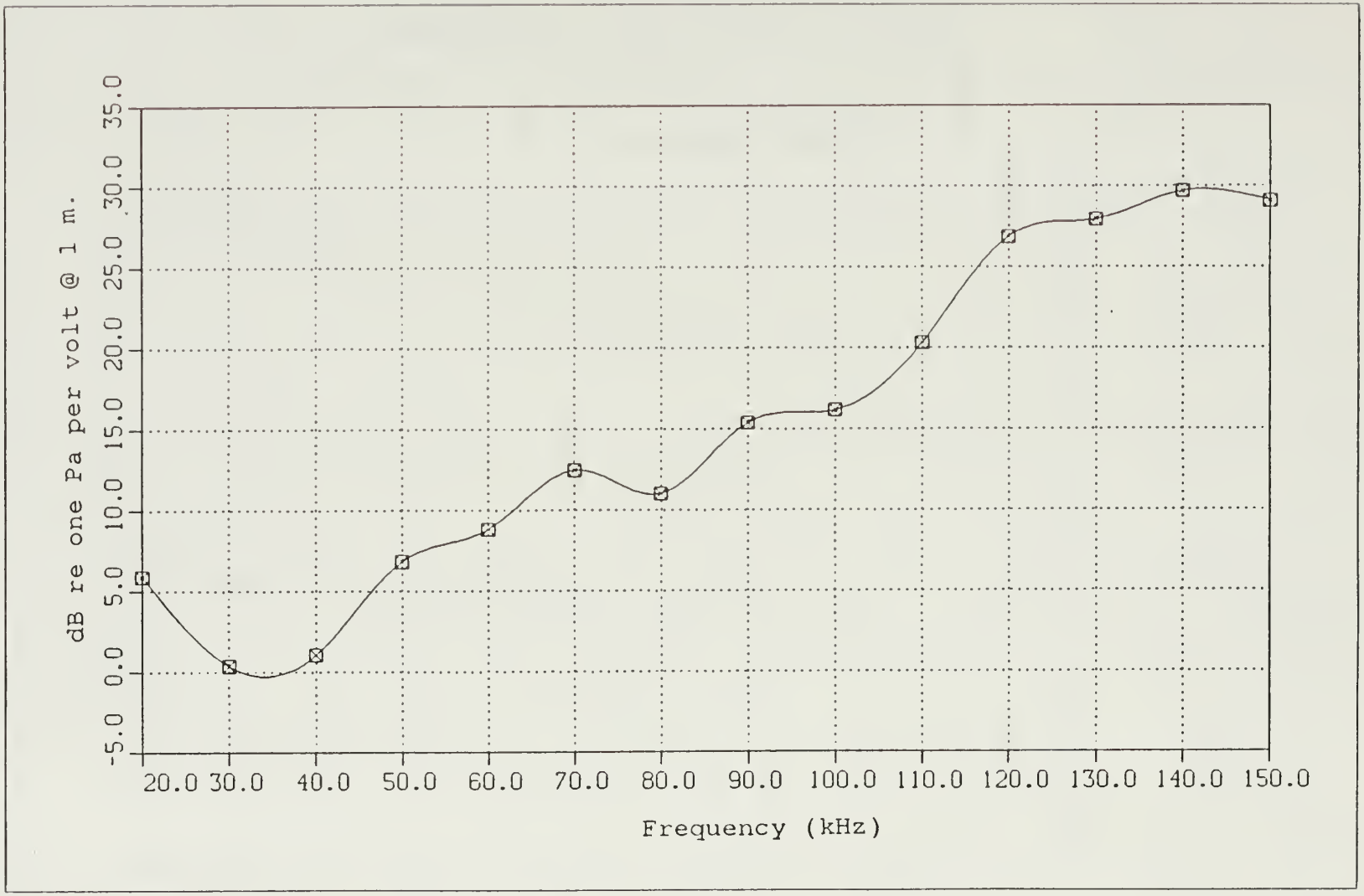

Figure 3.3 Voltage response of transducer.

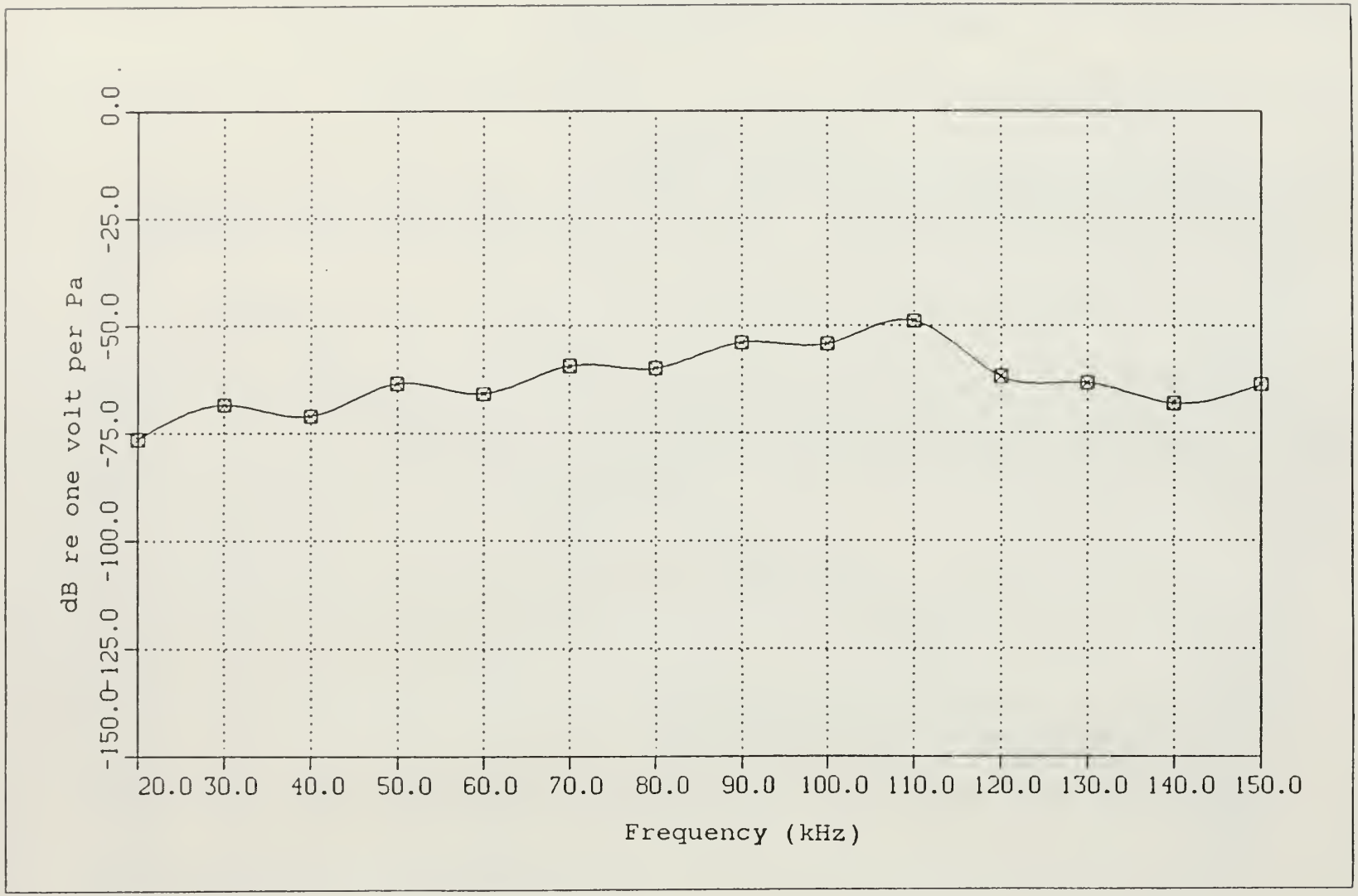

Figure 3.4 Sensitivity of receiver.

E. VALIDATION

To insure that the sound fields set up in the tank would be good approximations of the sound fields in the absence of sides and bottom (e.g, a shallow water environment of infinite horizontal extent), measurement were made on the sound field set up in the water and in the sand for a source in the water layer.

1. Sound Pressure as a Function of Receiver Depth

Figure 3.5 shows the circuit arrangement for the measurement of the variation of pressure amplitude with range and depth. Continuous waves of the desired frequency were generated by a frequency generator and were applied to the source through an amplifier. The source was placed at mid depth in the water layer which was 2.7 cm thick. The signal was received by the receiver and was passed through the bandpass filter to eliminate noise. The output from the bandpass filter was amplified and displayed on the oscilloscope. To determine the variations of pressure amplitude as a function of receiver depth, the transmitter was kept at a constant depth in the water layer while the measurements were made with the receiver at a fixed range beginning from the top surface of the water layer down into the bottom layer in steps of 0.5 centimeter. Three frequencies between the cut-offs of two first modes were selected for measurements. The data are tabulated in Tables V, VI, and VII and plotted in Figures 3.6, 3.7, and 3.8 . The experimental and theoretical results agree satisfactorily within the water layer. Near the cut-off frequency of the propagating mode, the experimental amplitude appears to decay more rapidly with depth in the bottom layer than theory predict. Decay is slower for intermediate and high frequencies.

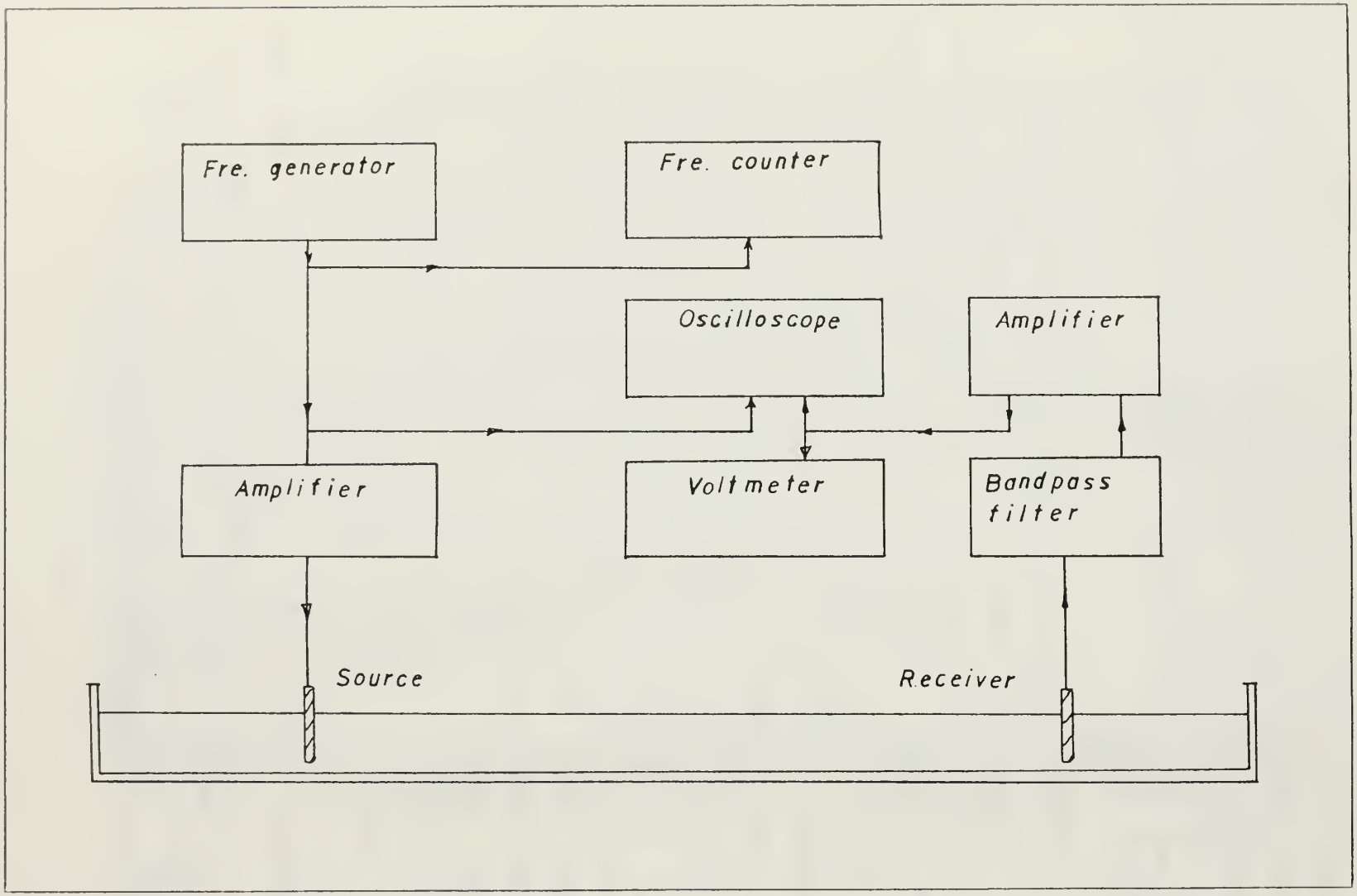

Figure 3.5 Measurement of pressure variations with range and depth.

TABLE V

Sound pressure as function of depth:
f = 35 kHz, n = 1, L = 1.5 m

No.	Depth(cm)	Volts	Normalized
1	0.0	0.012	0.12
2	0.5	0.028	0.28
3	1.0	0.056	0.56
4	1.5	0.081	0.81
5	2.0	0.097	0.97
6	2.5	0.1	1.0
7	3.0	0.097	0.97
8	3.5	0.083	0.83
9	4.0	0.067	0.67
10	4.5	0.052	0.52
11	5.0	0.042	0.42
12	5.5	0.041	0.41
13	6.0	0.038	0.38
14	6.5	0.034	0.34
15	7.0	0.028	0.28
16	7.5	0.023	0.23
17	8.0	0.018	0.18
18	8.5	0.015	0.15
19	9.0	0.016	0.16

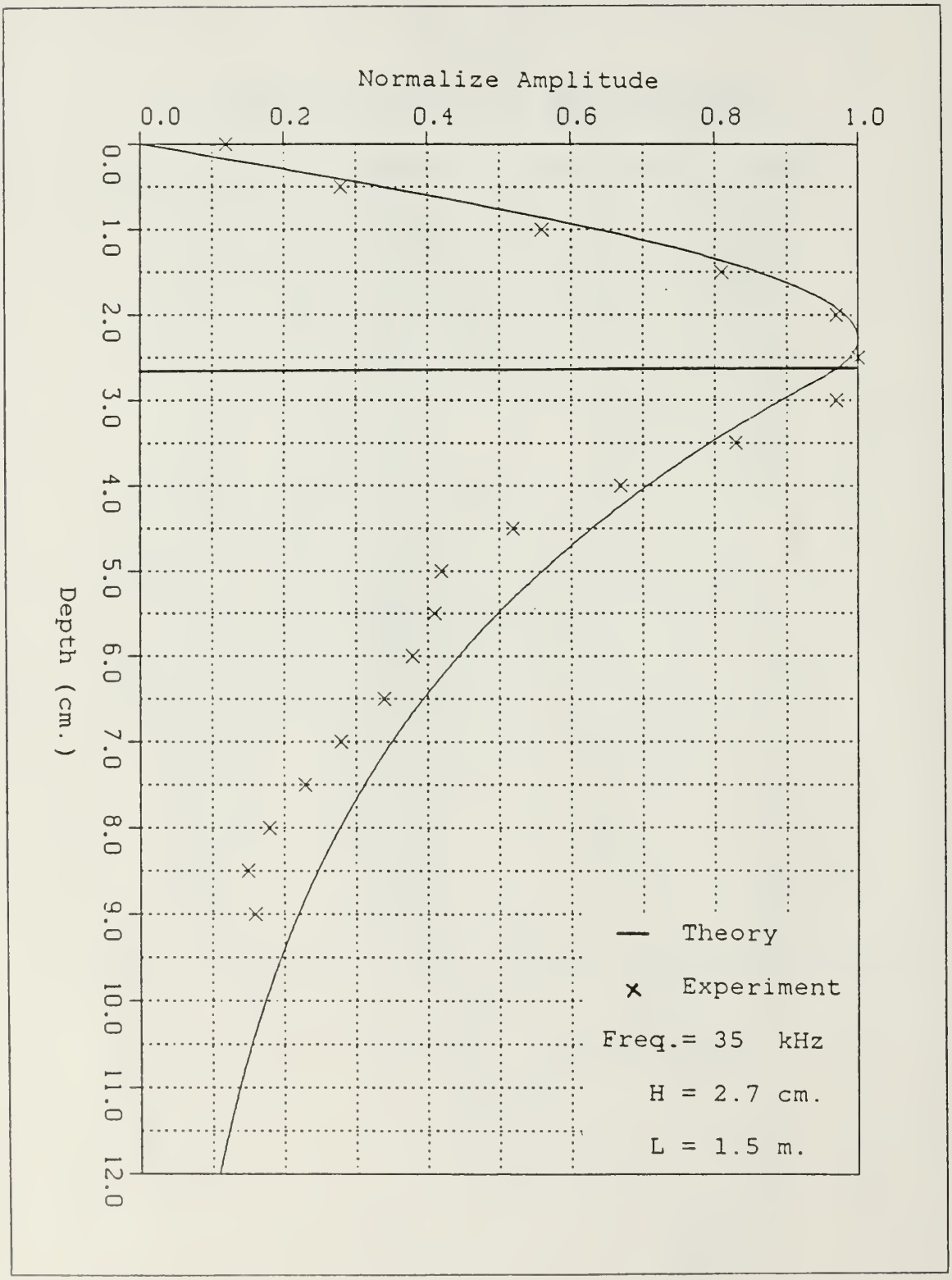

Figure 3.6 Pressure variation as function of receiver depth: f = 35 kHz n = 1.

TABLE VI

Sound pressure as function of depth:
f = 50 kHz, n = 1, L = 1.5 m

No.	Depth(cm)	Volts	Normalized
1	0.0	0.04	0.06
2	0.5	0.21	0.31
3	1.0	0.41	0.61
4	1.5	0.58	0.87
5	2.0	0.67	1.0
6	2.5	0.65	0.97
7	3.0	0.58	0.87
8	3.5	0.435	0.65
9	4.0	0.34	0.51
10	4.5	0.245	0.37
11	5.0	0.15	0.22
12	5.5	0.1	0.15
13	6.0	0.063	0.09
14	6.5	0.05	0.07
15	7.0	0.05	0.07
16	7.5	0.047	0.07
17	8.0	0.027	0.04
18	8.5	0.02	0.03
19	9.0	0.04	0.06

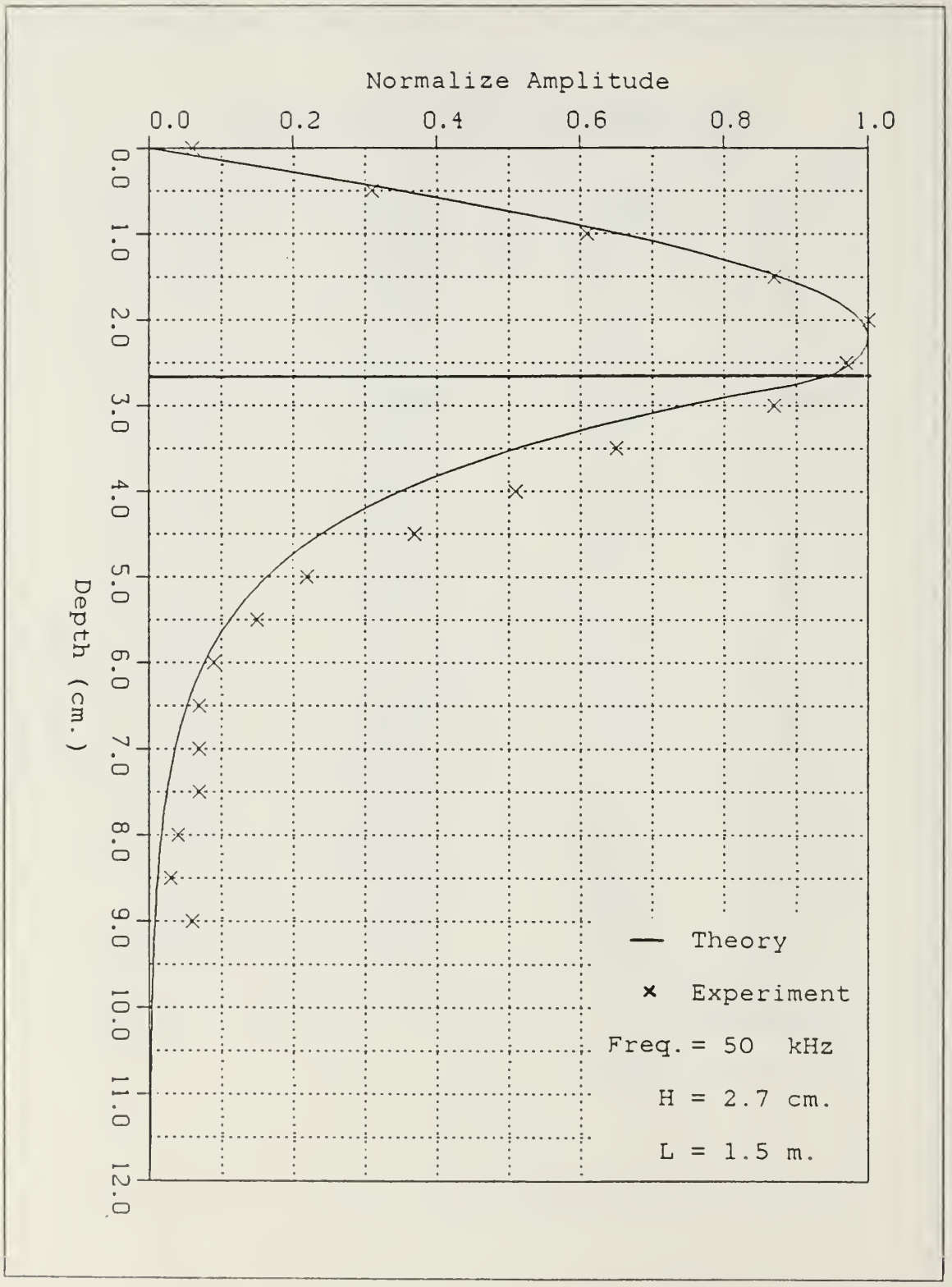

Figure 3.7 Pressure variation as function of receiver depth: f = 50 kHz n = 1.

TABLE VII

Sound pressure as function of depth:
f = 70 kHz, n = 1, L = 2.0 m

No.	Depth(cm)	Volts	Normalized
1	0.0	0.095	0.05
2	0.5	0.53	0.28
3	1.0	1.15	0.6
4	1.5	1.7	0.89
5	2.0	1.9	1.0
6	2.5	1.75	0.92
7	3.0	1.2	0.63
8	3.5	0.7	0.37
9	4.0	0.24	0.13
10	4.5	0.205	0.11
11	5.0	0.2	0.1
12	5.5	0.195	0.1
13	6.0	0.13	0.07
14	6.5	0.043	0.02
15	7.0	0.06	0.03
16	7.5	0.065	0.03
17	8.0	0.1	0.05
18	8.5	0.105	0.055
19	9.0	0.073	0.04

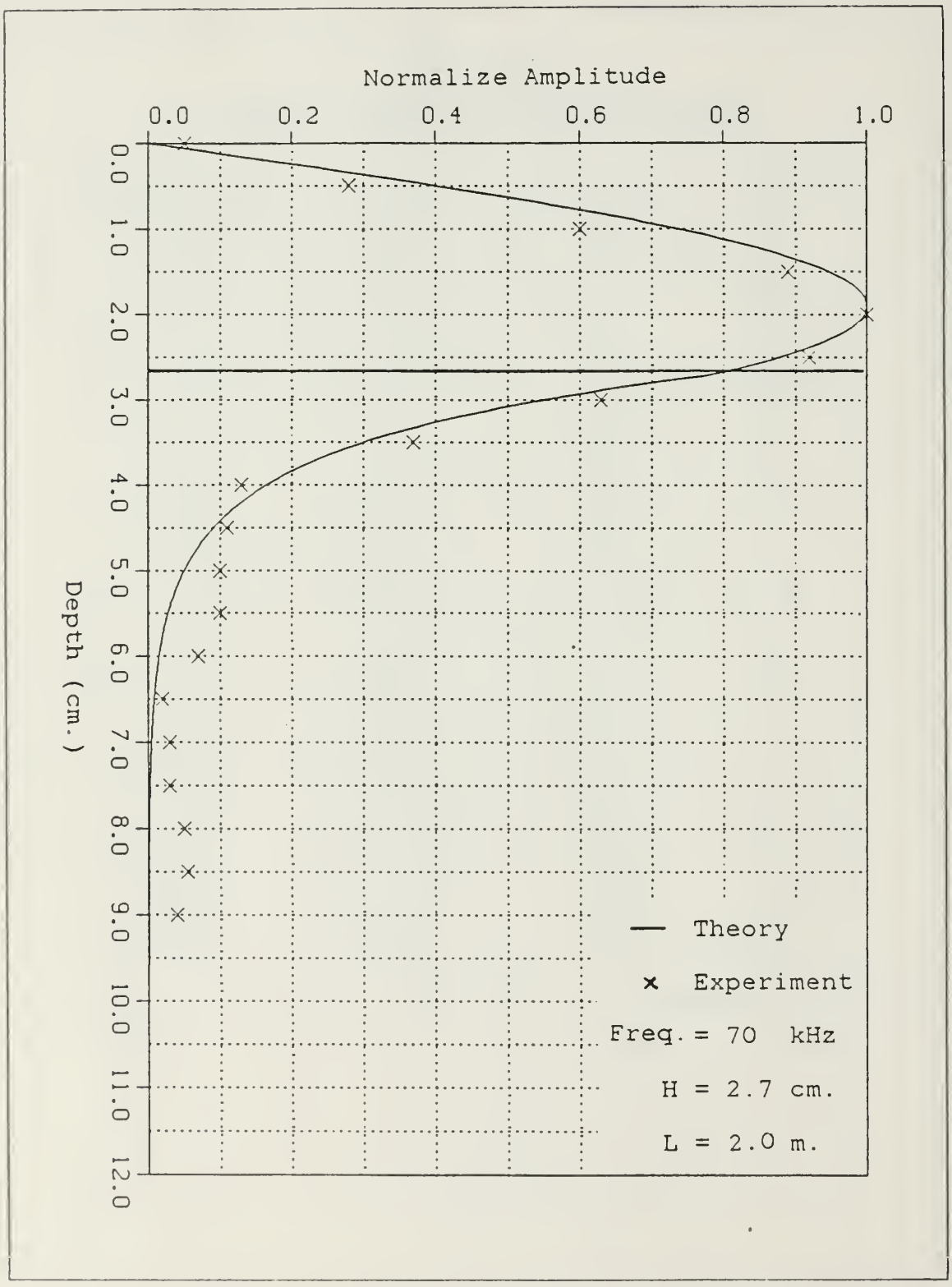

Figure 3.8 Pressure variation as function of receiver depth: f = 70 kHz n = 1.

2. Sound Pressure as a Function of Range

To measure the variation of peak pressure amplitude with range, the transmitter was kept at constant depth and the receiver's depth was adjusted slightly at each range to measure peak amplitude at that range. Precautions had to be taken to ensure that the water surface is disturbed as little as possible because variation in water depth had a significant effect on the pressure amplitude. Measurements were made for three frequencies between the cut-offs of the first two modes. The data are tabulated in Tables VIII, IX, and X and is plotted in Figures 3.9, 3.10, and 3.11 respectively. Assuming a simple model for which the loss in the bottom effects that portion of the energy density of the normal mode found in the bottom, which then "robs" the energy density in the water layer, then the effective absorption coefficient can be estimated as (Ref. personal communication with Prof. Alan B. Coppens)

$$\alpha \approx \frac{1}{4} F \frac{A_b}{A} \qquad \text{dB/m}$$

Where A_b/A is fraction of the energy density of the normal mode in the bottom and 1/4F (F is the frequency in kHz) yields the expected attenuation to be found in the sand used for the bottom [Ref. 4]. Comparison of the measured data with the simplestic model is very good, suggesting that indeed the sound field is subjected to minimal effects from the side walls.

TABLE VIII

Sound pressure as function of range:
H = 2 cm f = 50 kHz n = 1

No.	Distance(m)	Volts	Normalized
1	1.00	0.45	1.0
2	1.25	0.34	0.756
3	1.50	0.255	0.567
4	1.75	0.195	0.433
5	2.00	0.2	0.444
6	2.25	0.168	0.373
7	2.50	0.108	0.24
8	2.75	0.155	0.344
9	3.00	0.105	0.233
10	3.25	0.078	0.173
11	3.50	0.022	0.049
12	3.75	0.047	0.104
13	4.00	0.059	0.131
14	4.25	0.057	0.127
15	4.50	0.043	0.095
16	4.75	0.042	0.093
17	5.00	0.031	0.069

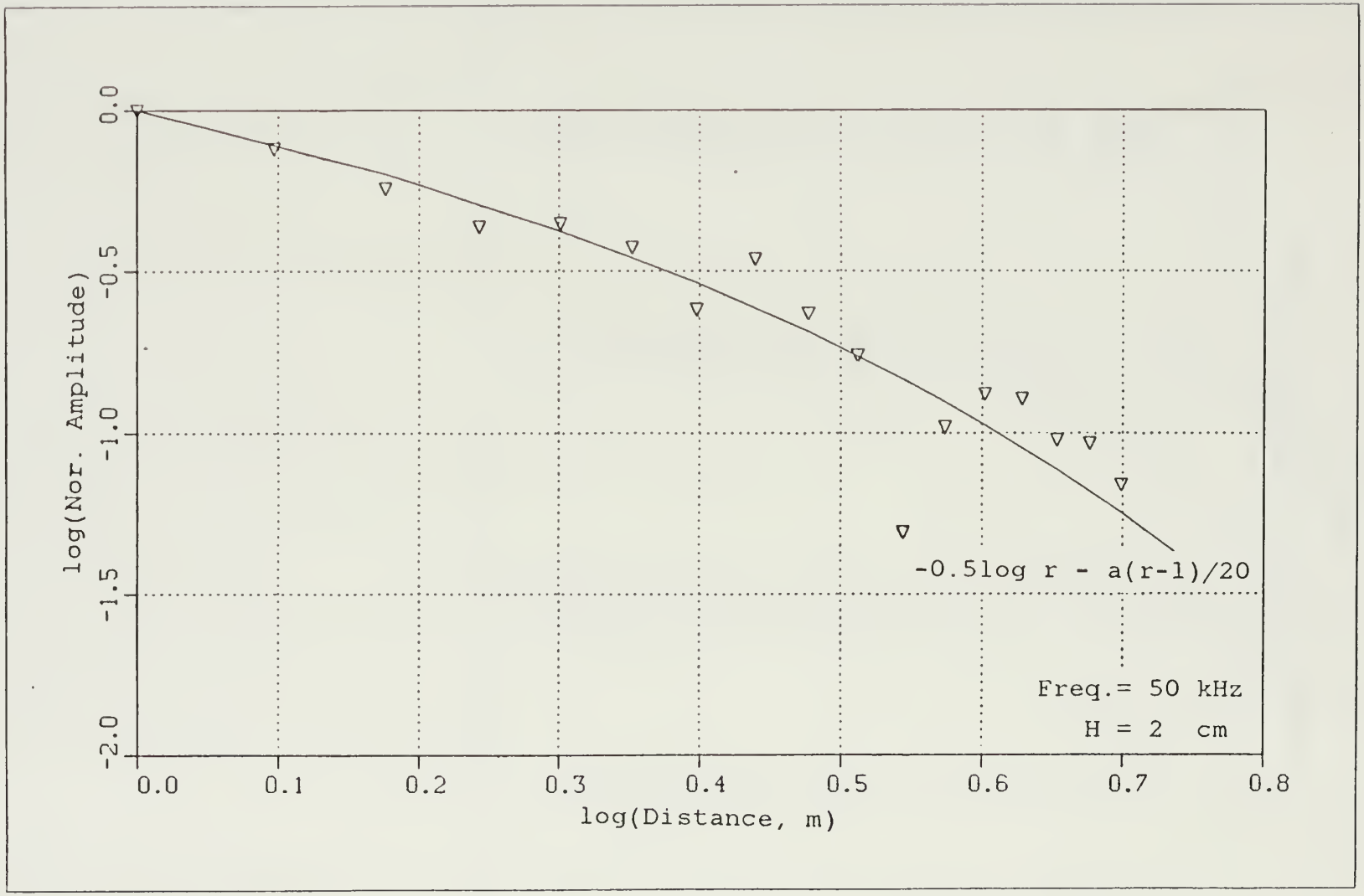

Figure 3.9 Sound pressure variation as function of range: f = 50 kHz n = 1.

TABLE IX

Sound pressure as function of range:
H = 2 cm f = 70 kHz n = 1

No.	Distance(m)	Volts	Normalized
1	1.00	2.08	1.0
2	1.25	1.6	0.769
3	1.50	1.7	0.817
4	1.75	1.0	0.481
5	2.00	0.93	0.447
6	2.25	1.1	0.529
7	2.50	0.85	0.409
8	2.75	0.68	0.327
9	3.00	0.87	0.418
10	3.25	0.62	0.298
11	3.50	0.17	0.082
12	3.75	0.61	0.293
13	4.00	0.58	0.279
14	4.25	0.36	0.173
15	4.50	0.315	0.151
16	4.75	0.3	0.144
17	5.00	0.29	0.139

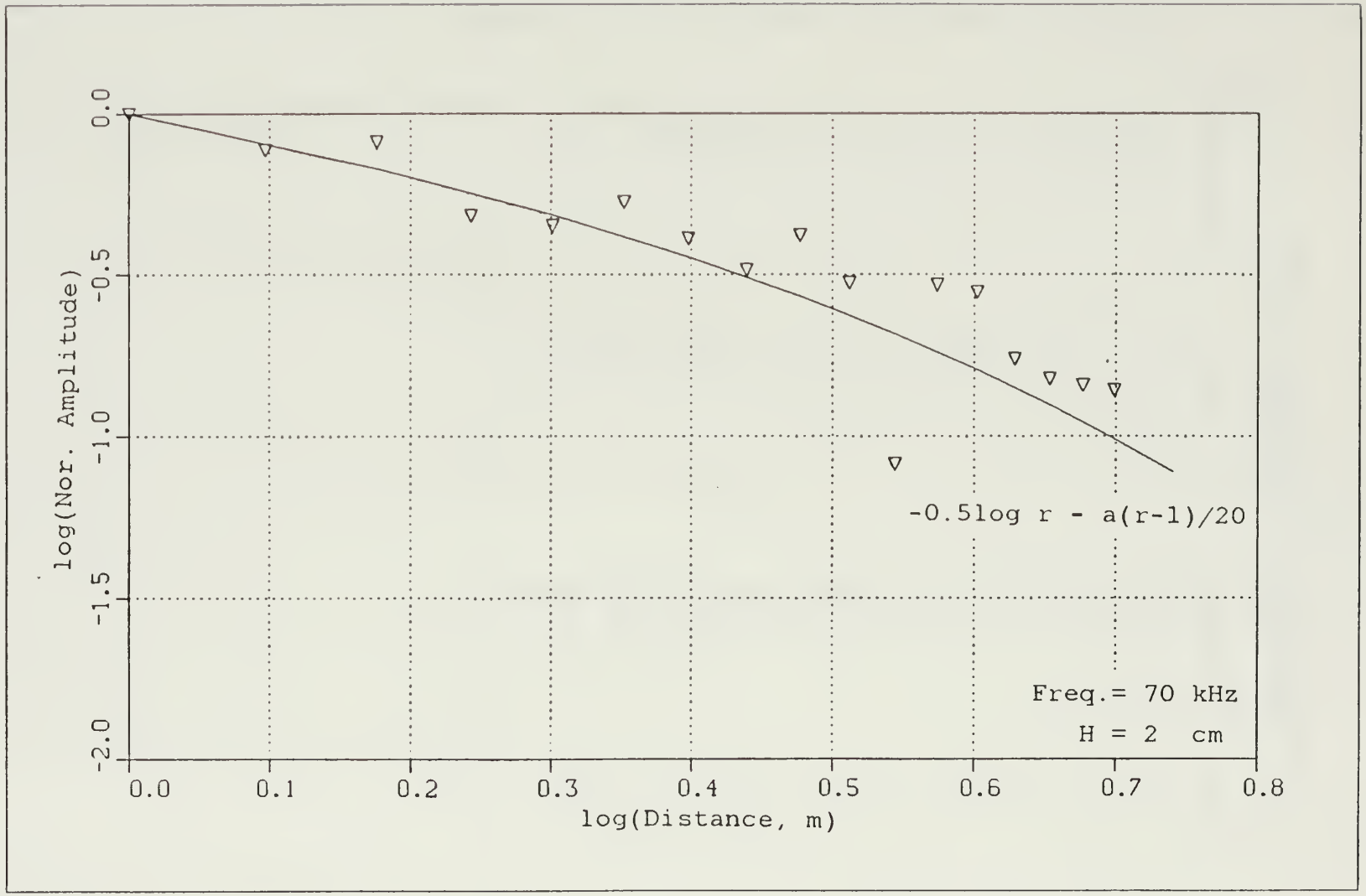

Figure 3.10 Sound pressure variation as function of range: f = 70 kHz n = 1.

TABLE X

Sound pressure as function of range:
H = 2 cm f = 100 kHz n = 1

No.	Distance(m)	Volts	Normalized
1	1.00	1.95	1.0
2	1.25	1.4	0.718
3	1.50	1.4	0.718
4	1.75	1.05	0.538
5	2.00	1.0	0.513
6	2.25	0.88	0.451
7	2.50	0.83	0.426
8	2.75	0.85	0.436
9	3.00	0.74	0.379
10	3.25	0.63	0.323
11	3.50	0.7	0.359
12	3.75	0.28	0.144
13	4.00	0.65	0.333
14	4.25	0.5	0.256
15	4.50	0.41	0.21
16	4.75	0.49	0.251
17	5.00	0.41	0.21

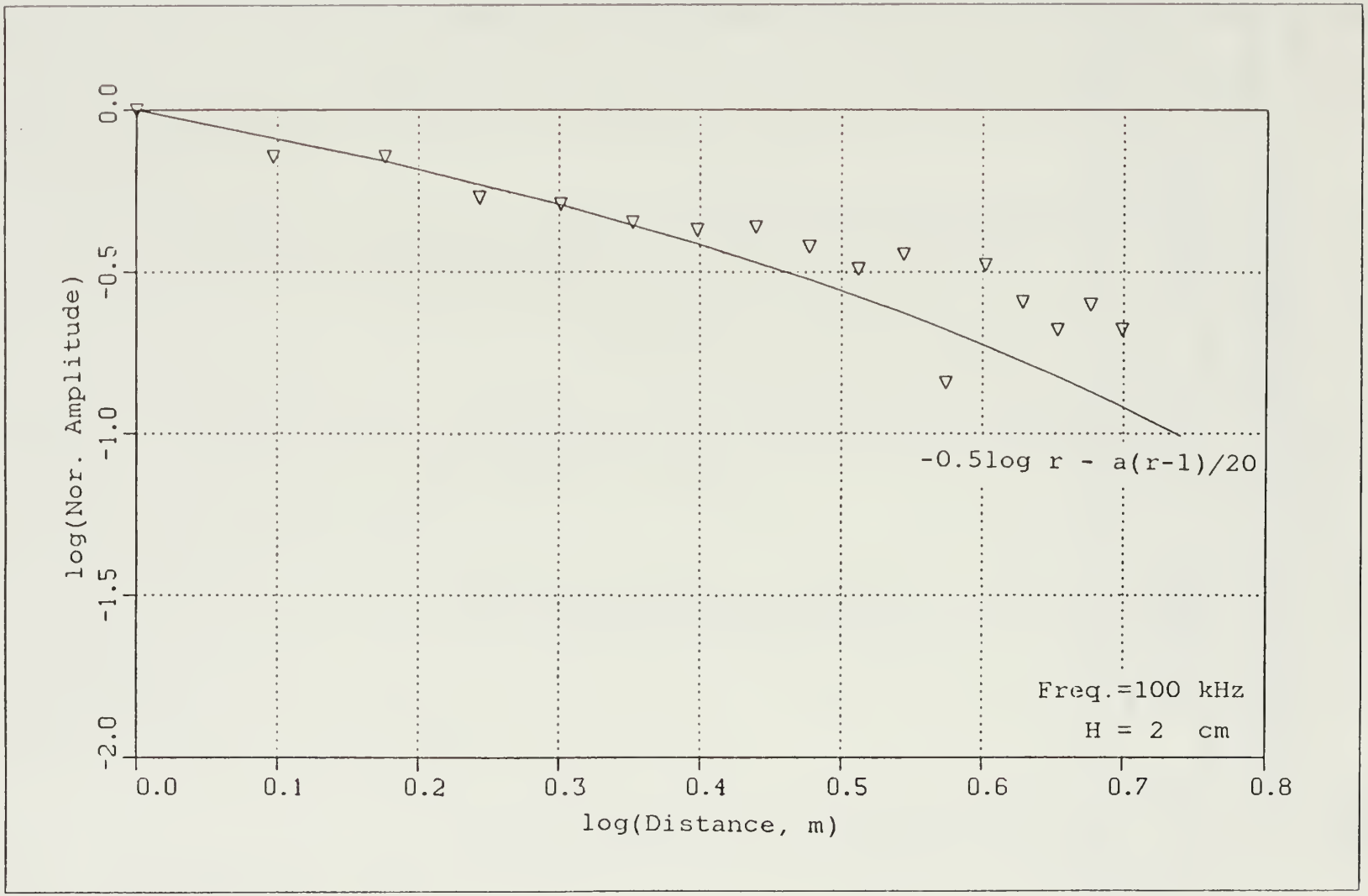

Figure 3.11 Sound pressure variation as function of range: f = 100 kHz n = 1.

3. Sound Pressure Variation Across the Width of the Tank

Sound pressure variations were measured across the width of the tank at a one meter distance from the source for three different frequencies. The measured data shown in Table XI, XII, and XIII and plotted in Figures 3.12, 3.13, and 3.14. The results show slight effects of interference either from the walls or from the bottom of the sand layer.

TABLE XI

Transverse measurement of sound pressure:
f = 50 kHz, L = 1 m

Distance (cm)	Volts	Distance (cm)	Volts
-32	0.38	-3.5	0.4
-30.5	0.215	-1.7	0.55
-29	0.38	0	0.40
-27.5	0.34	2	0.55
-26.4	0.39	4	0.4
-25.2	0.32	6.7	0.53
-23.7	0.47	8.5	0.34
-22	0.33	10.7	0.49
-20	0.5	13.8	0.36
-18	0.33	16.3	0.49
-16.3	0.5	18.8	0.32
-15	0.42	20.2	0.4
-13.5	0.5	22.2	0.31
-11.8	0.36	23.5	0.38
-9.9	0.53	24.7	0.33
-7.2	0.42	26	0.37
-5.3	0.53	27.7	0.25

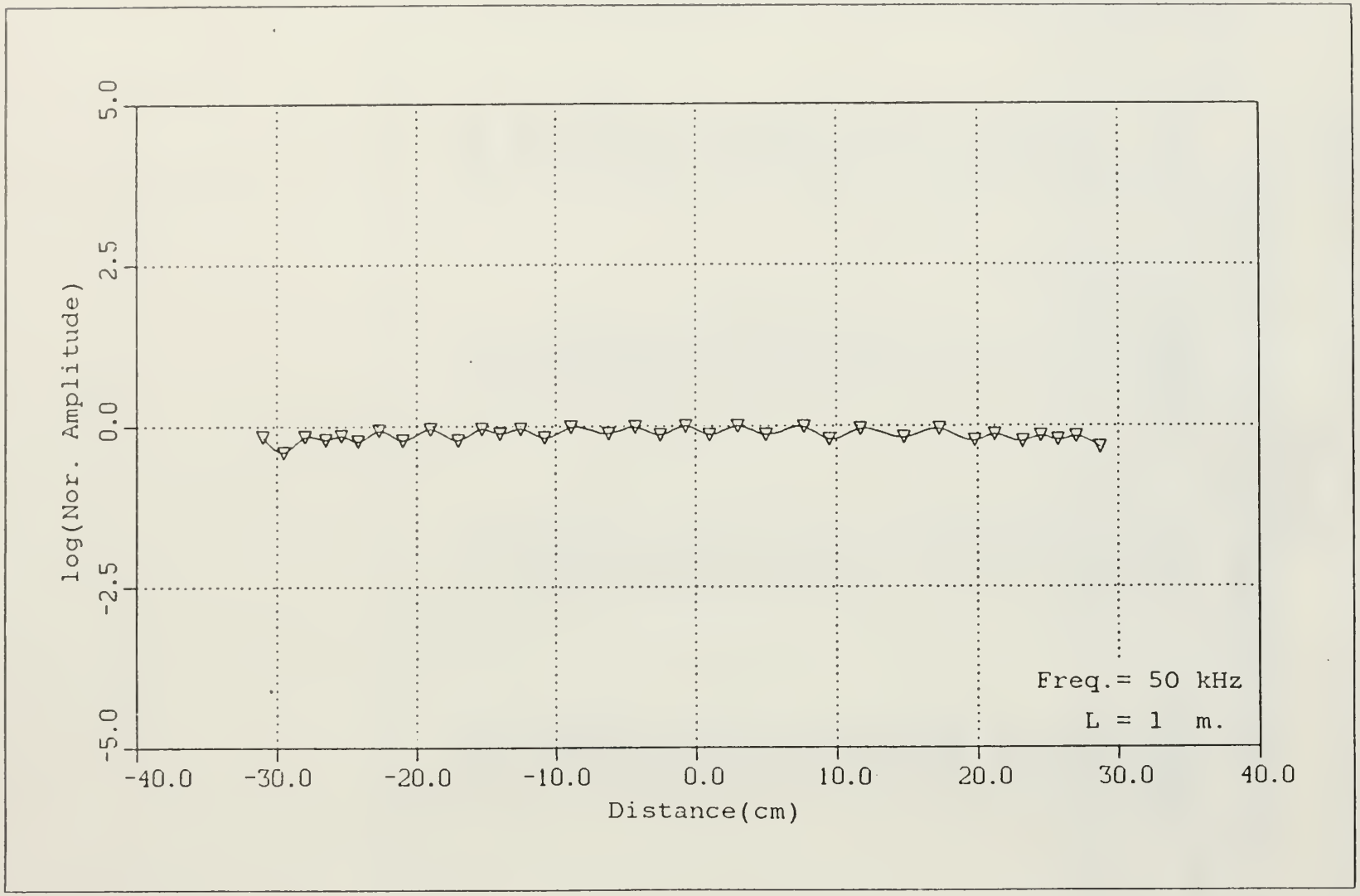

Figure 3.12 Transverse variation of sound pressure: f = 50 kHz, L = 1 m.

TABLE XII

Transverse measurement of sound pressure:
f = 70 kHz, L = 1 m

Distance (cm)	Volts	Distance (cm)	Volts
-32	1.7	-1.3	1.7
-30.6	1.25	0.4	2.47
-29.4	1.4	2	1.6
-28.6	1.25	3.7	2.17
-27.2	1.8	5.2	1.35
-26	1.25	7	2.23
-24.9	1.75	8.7	1.45
-23.7	1.2	10	2.12
-22.5	2.05	11	1.85
-21.3	1.2	12.3	2.2
-19.8	2.2	13.7	1.4
-18.4	1.5	15	2.1
-16.8	1.9	16.5	1.65
-15.6	1.7	17.8	1.9
-14.2	2.1	18.8	1.57
-13.3	1.82	19.8	1.75
-12	1.98	21.2	1.3
-10.7	1.75	22.5	1.62
-9.2	2.2	23.6	1.35
-7.8	1.55	24.5	1.6
-6	2.5	26	1.0
-4.5	1.65	27.8	1.5
-3	2.32		

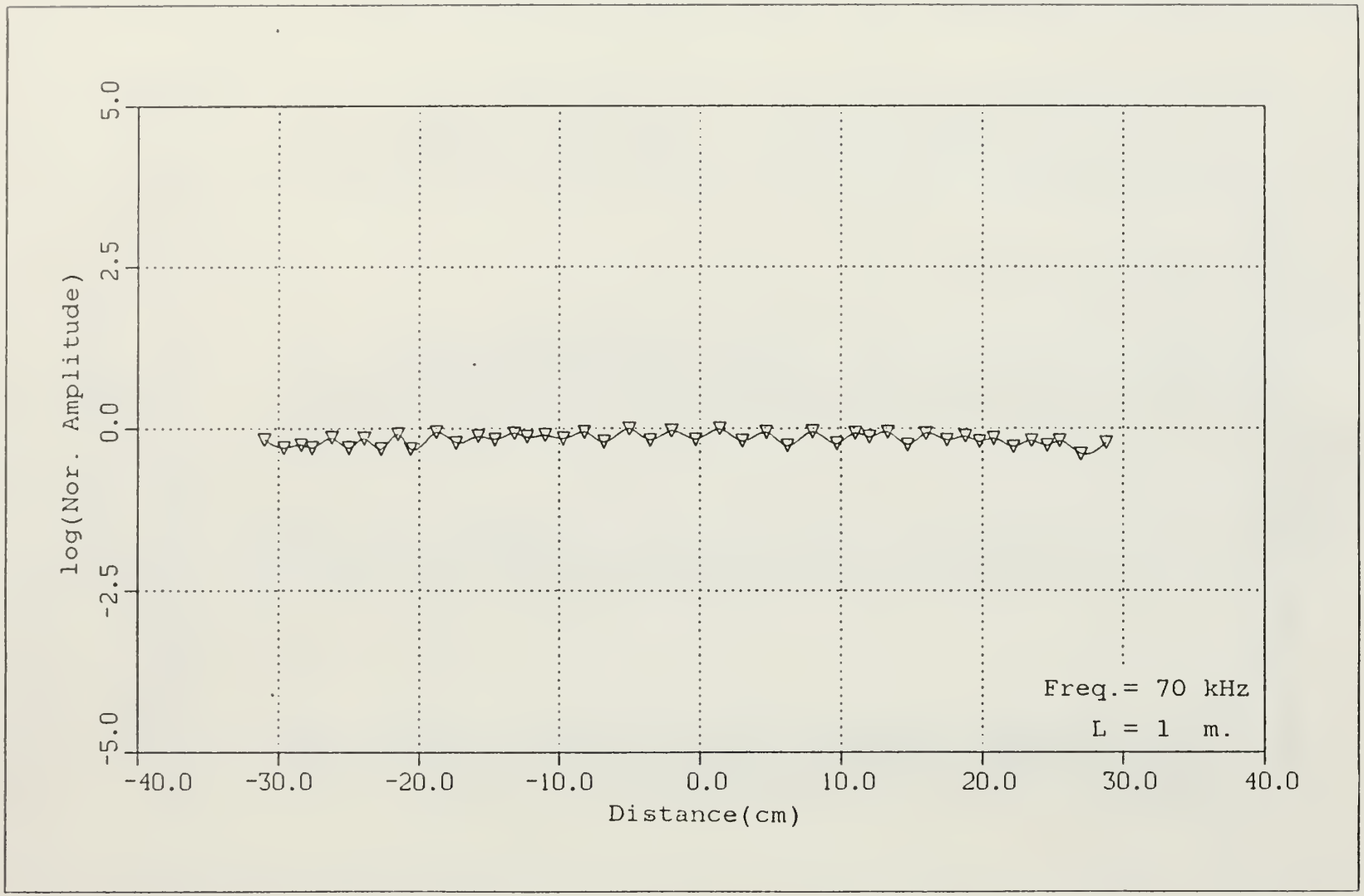

Figure 3.13 Transverse variation of sound pressure: f = 70 kHz, L = 1 m.

TABLE XIII

Transverse measurement of sound pressure:
f= 100 kHz, L = 1 m

Distance (cm)	Volts	Distance (cm)	Volts
-32	1.25	-4	1.47
-30.8	0.82	-1.9	1.9
-29.6	1.5	-0.4	1.52
-28.4	0.94	0.5	1.7
-27	1.4	1.5	1.6
-25.5	0.94	2.4	1.7
-23.8	1.62	3.4	1.62
-22.6	1.15	5.3	1.22
-20.5	1.76	7.8	1.67
-18.7	1.55	10	1.1
-17.5	1.8	12.5	1.35
-16.4	1.5	15.6	0.82
-15.4	1.9	16.5	1.22
-14.4	1.5	18	0.63
-13.5	1.8	19.8	1.05
-13	1.6	21.2	0.67
-11.7	2.2	22.5	0.95
-10.7	1.65	24.7	0.49
-9.5	1.8	26	0.68
-8.7	1.65	27.5	0.42
-7	1.88		

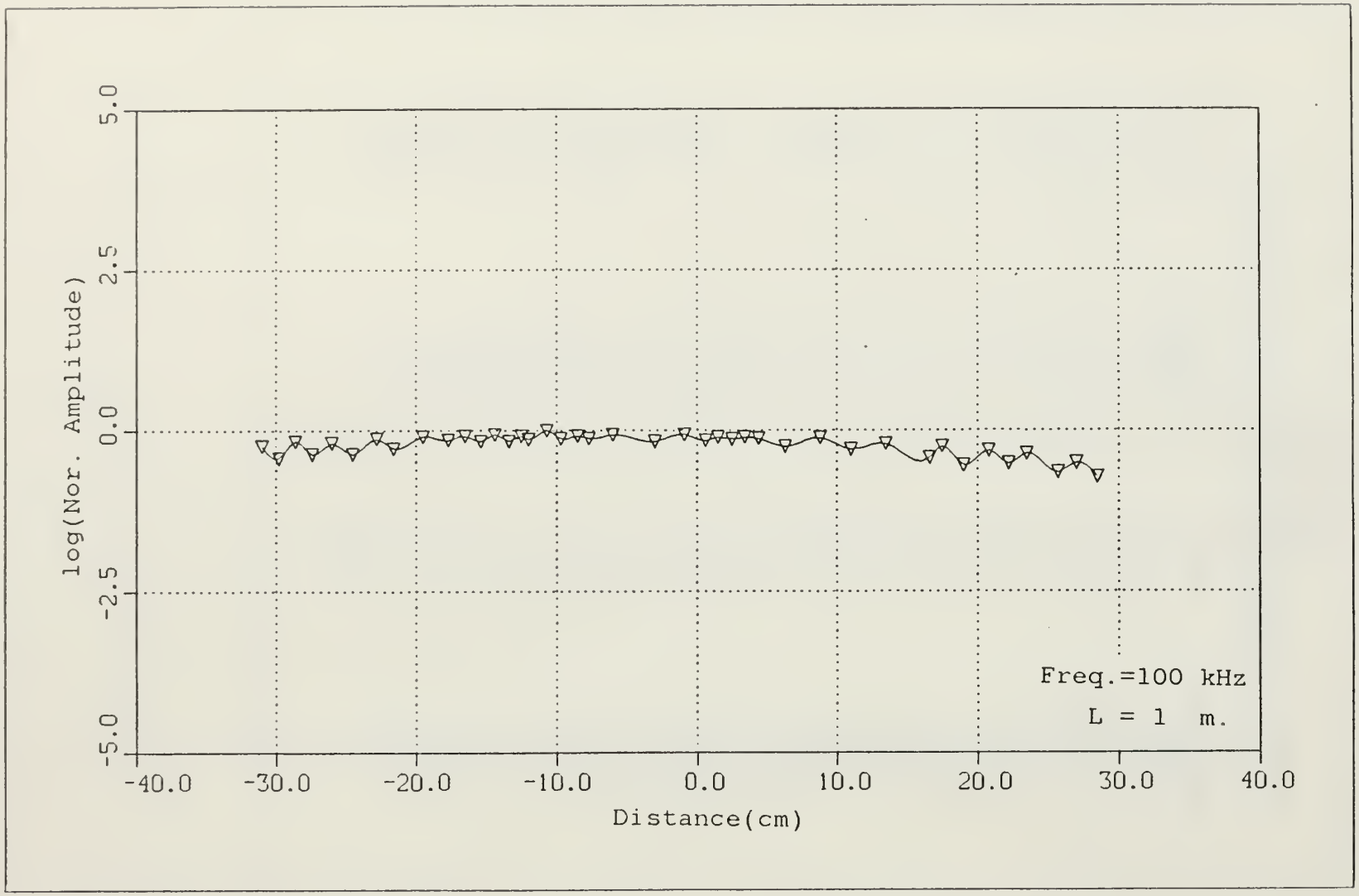

Figure 3.14 Transverse variation of sound pressure: f = 100 kHz, L = 1 m.

F. SUMMARY AND CONCLUSION

In the preceding sections, the experimental curves for the pressure amplitude as a function of depth and range for three different frequencies for which only the first normal mode propagates have been compared with normal mode theory and a simple model for attenuation of the normal mode. The depth dependent curves both in the water and in the sand agrees satisfactorily with the theory. The range dependence obtained in the water exhibit excellent agreement with the simple modeling of losses resulting from the relatively highly attenuating bottom. Measurements both in range and transverse dimensions suggests that the sound field is subjected to minimal effects from the side walls. The leveling arrangement needs improvement because at higher frequencies minor alterations in water depth changes the pressure amplitude considerably.

LIST OF REFERENCES

1. C. Allan Boyles, Acoustic Waveguides, Wiley, New York(1984).

2. L.E. Kinsler, A.R. Frey, A.B. Coppens, and J.V. Sanders, Fundamental of Acoustics, 3rd Edition, Wiley, New York(1982).

3. C.L. Pekeris, Theory of Propagation of Explosive Sound in Shallow Water, (Geological Society of America Memoir 27, October 1948)

4. Robert J. Urick, Principles of Underwater Sound, McGraw-Hill, New York (1983)

INITIAL DISTRIBUTION LIST

No.		Copies
1.	Defense Technical Information Center Cameron Station Alexandria, Virginia 22314	2
2.	Library, Code 0142 Naval Postgraduate School Monterey, California 93943	2
3.	LT.CDR. Mohammad Tariq P.N. Block No.12E, Flat No.4 NORE-I Moulvi Tamizuddin Khan Road Karachi, Pakistan	3
4.	ENS. Suttichai Rungsirotekomol R.T.N. 337 Sukhumvit 103 Prakanong Bangna Bangkok (10260), Thailand	3
5.	Superintendent ATTN: Dr. J. V. Sanders, Code 61Sd Naval Postgraduate School Monterey, California 93943	5
6.	Superintendent ATTN: Dr. A. B. Coppens, Code 61Cz Naval Postgraduate School Monterey, California 93943	2
7.	Superintendent ATTN: LCDR C. R. Dunlap, USN(Ret), Code 68Di Naval Postgraduate School Monterey, California 93943	1
8.	Chief of Naval Research ATTN: Dr. Michael McKissick 800 N. Quincy St. Arlington, Virginia 22217	1
9.	Chief of Naval Research ATTN: Dr. Raymind Fitzcerald 800 N. Quincy St. Arlington, Virginia 22217	1
10.	Dr. F. H. Fisher Marine Physical Laboratory University of California at San Diago San Diago, California 92110	1
11.	Eugene W. Brown NAVOCEANO Code 7300 Bay St. Louis, Ms. 39522	1
12.	Commanding Officer ATTN: Dr. James Andrews Naval Ocean Research and Development Activity NSTL Station Bay St. Louis, Ms. 39522	1

213145

Thesis
T1385 Tariq
c.1 Propagation of
sound in a layered
laboratory model.